TAMPEREEN TEKNILLINEN YLIOPISTO
TAMPERE UNIVERSITY OF TECHNOLOGY

TANELI HEIKKILÄ

FATIGUE LIFE IMPROVEMENT OF A WELDED STRUCTURE WITH TOPOLOGY OPTIMIZATION

Master's thesis

Examiner: Assoc. Prof. Sami Pajunen
Examiner and topic approved by the Faculty Council of the Faculty of Engineering Sciences on 3rd January 2018

ABSTRACT

TANELI HEIKKILÄ: Fatigue life improvement of a welded structure with topology optimization.
Tampere University of Technology
Master of Science Thesis, 72 pages, 2 Appendix pages
December 2017
Master's Degree Programme in Mechanical Engineering
Major: Analysis of Machines and Structures
Examiner: Associate Professor Sami Pajunen

Keywords: Fatigue analysis, Topology optimization, Palmgren-Miner cumulative fatigue damage, Effective notch stress

This master's thesis deals with topology optimization as a tool for fatigue life improvement of a welded structure. Welded structures are prone to failure due to fatigue caused by cyclic loads. Optimizing structures against fatigue with topology optimization has very few practical examples in literature, but it has proven as promising technique.

In this work we utilize rainflow cycle counting method, Palmgren-Miner damage sum and effective notch stress method to create constraint function for weld seam fatigue stress to attain optimal design in terms of fatigue strength and stiffness.

The method was then adapted on Ponsse C44+ parallel crane boom head design to improve fatigue life of the structure. Structure was optimized using ANSYS and GENESIS topology optimization software with custom made fatigue constraint function. Results show significant reduction on stress ranges at the weld seam.

TIIVISTELMÄ

TANELI HEIKKILÄ: Hitsatun rakenteen väsymiskestoiän parantaminen topologiaoptimoinnilla.
Tampereen teknillinen yliopisto
Diplomityö, 72 sivua, 2 liitesivua
Joulukuu 2017
Konetekniikan diplomi-insinöörin tutkinto-ohjelma
Pääaine: Koneiden ja rakenteiden analysointi
Tarkastaja: Associate Professor Sami Pajunen

Avainsanat: Väsymisanalyysi, topologiaoptimointi, Palmgren-Miner vauriosumma, tehollinen lovijännitys

Tässä diplomityössä tutkittiin topologiaoptimoinnin soveltamista rakenteen väsymiskestoiän parantamiseen. Hitsatut rakenteet ovat herkkiä syklisen kuormituksen aiheuttamalle väsymiselle. Topologiaoptimoinnin soveltamisesta käytännön väsymiskestoiän parantamiseen ei ole juurikaan julkaisuja, mutta se on osoittautunut lupaavaksi menetelmäksi.

Optimointia varten luotiin väsymisrajoitusehto-funktio käyttäen rainflow kuormitussyklien laskentaa, Palmgren-Minerin vauriosumma menetelmää ja tehollisen lovijännityksen menetelmää.

Väsymisrajoitusehtoa sovellettiin Ponssen C44+ nostopuomin valupään optimointiin väsymiskestoiän parantamiseksi. Optimointiin käytettiin ANSYSta ja GENESIksen topologiaoptimointiohjelmistoa. Tuloksena saatiin uusi puominpää, jossa hitsisauman jännitykset ovat merkittävästi matalammat kuin alkuperäisessä rakenteessa.

PREFACE

I would like to thank Ponsse Oyj for offering me such an interesting subject to work on. Ponsse has supported me through the project by offering all the required software and tools I have needed, making the work a pleasure. The subject has allowed me to increase my knowledge on fatigue analysis to whole new level. I would also like to thank Marko Halonen, the facilitator of this project at Ponsse, for guiding me to right direction in the beginning of this project.

Taneli Heikkilä

Vieremä, December 2017

TABLE OF CONTENTS

LIST OF SYMBOLS AND ABBREVIATIONS

a	Initial crack size
a_i	Maximum acceptable crack size
BCC	Body centered cubic
BESO	Bi-directional Evolutional Structure Optimization
CA	Constant amplitude
CTL	Cut to length
C_0	Power law constant
da	Crack propagation
DOF	Degree of freedom
DSA	Dual sequential approximation
D_i	Damage sum above knee point
D_j	Damage sum below knee point
D_{limit}	Maximum specified damage sum
D_{spec}	Damage sum of the spectrum
$D_{spec.max}$	Maximum damage sum of one spectra
$D_{specified}$	Maximum acceptable damage sum
E	Young's modulus
ENS	Effective notch stress
EPFM	Elastic plastic fracture mechanics
E_{min}	Minimum elasticity tensor
E_0	Young's modulus of the material
FCC	Face centered cubic
FEA	Finite element analysis
$F(a)$	Correction factor for stress intensity factor
HAZ	Heat affected zone
HFMI	High frequency mechanical impact
IIW	International institution of welding
k	Slope of the S-N curve before knee point
k'	Slope of S-N curve after knee point
K_I	Stress intensity factor
K_{Ic}	Critical fracture toughness
LEFM	Linear elastic fracture mechanics
LTT	Low transformation temperature

$L_{spectra}$	Length of the spectrum
m	Material specific reduction constant for S-N curve
m_1	S-N curve slope above knee point
m_2	S-N curve slope below knee point
n	Stress scaling factor
n_i	Number of cycles above knee point
n_j	Number of cycles below knee point
N_p	Number of cycles to failure
$N_{service}$	Number of spectras
p	penalization factor
r	Averaging radius
SIMP	Solid Isotropic Material with Penalization method
t	Plate thickness
TO	Topology optimization
T_{sl}	Service life
UIT	Ultrasonic impact treatment
VA	Variable amplitude
x_e	Density variable
$X\,(x)$	Material distribution indicator
α	Geometrical parameter
Δ	Critical plane
ΔK_I	Cyclic load stress intensity factor
$\Delta\sigma_{\mathrm{a,eq}}$	Equivalent tensile stress range
$\Delta\sigma_{a,SN}(N)$	Hot spot fatigue stress limit at pure tension
$\Delta\sigma_{i,S,d}$	Stress range design value above knee point
$\Delta\sigma_{j,S,d}$	Stress range design value below knee point
$\Delta\sigma_{L,d}$	Stress range at knee point of S-N curve
l	Equivalent shear stress range
ε	Strain
ε_{hs}	Hot spot strain
ε_x	Strain in x-direction
ε_y	Strain in y-direction
ν	Poisson's ratio
σ_f	Failure stress
σ_{hs}	Hot spot stress

$\sigma_{0.4t}$	Stress at 0.4*t distance from weld edge
σ_{4mm}	Stress at 4 mm distance from weld edge
$\tau_{a,SN}(N)$	Hot spot fatigue stress limit at pure torsion
Ω	Design space

1. INTRODUCTION

Fatigue life assessment of structures has been major difficulty in engineering for decades. First writings in fatigue date back to late 19th century when serious problems were detected in railroads when axles of trains began failing. Since then fatal failures have occurred in for example airplanes and large vessels of which most well-known are Aloha Airlines Flight 243 and World War II era liberty vessels, notorious for fatal fatigue fracture. In this thesis we give brief overview of fatigue phenomena in welded structures and go through general guidelines of practical methods for engineers to use in design and analysis against fatigue.

To be able to fully understand all the elements of fatigue, overview of fatigue phenomena is given. Most common practical fatigue life determination methods for welded structures are also explained and some recent work on the field of fatigue life determination are addressed. Set of chosen methods are then used in case study where a part of forest machine boom is optimized against fatigue life.

The aim of this thesis is to find improved design for harvester boom head in terms of fatigue life. This problem will be assessed by design and topology optimization methods paired with fatigue analysis. Novelty of this thesis lies in combining fatigue constraint into topology optimization. Some promising results have been achieved with this technique on academic examples in this decade, but practical industrial examples are yet to be tested. Combining fatigue constraint into topology optimization effectively, should result quickly into new designs with improved fatigue properties, while still fulfilling other design constraints.

This thesis begins with brief history of fatigue and the development of the theories of fatigue and more in the fatigue phenomena in welded structures. In section 3 the various methods of fatigue life analysis are explained. The section is split in sub-sections describing the main steps into fatigue life assessment of a welded structure. Section 4 gives explanation of fatigue life improvement techniques to consolidate the understanding of driving factors on weld fatigue.

In the section 5 the theory of topology optimization is explained. In this section thorough introduction to topology optimization with solid isotropic material with penalization method is given with insight to practical usage of GENESIS topology optimization.

Finally in section 6 we introduce a case study which is to be addressed in this thesis. After introducing the case study, explanation of the operation of cut to length harvester forest

machine is given in section 7. The theories presented in earlier sections are applied into the case study in the final sections. Acceptable stress level is evaluated in section 8, the flow and steps of the optimization task is explained in section 9 and finally the results are given in section 10.

The thesis is finished in section 11 with conclusion including the proposed new structure, observations and problems found during optimization writers' ideas of future work that should be done on field of fatigue analysis to improve the results. Work is summed up in section 12.

2. FATIGUE

Fatigue of steel structures is driven by metal fracture phenomenon. Fracture is ultimately phenomenon where constantly applied stress breaks an atomic bond between two atoms. In typical steel structure the crack initiation, crack propagation and ultimately failure has been investigated broadly. The fracture process and corresponding factors are displayed in figure 1.

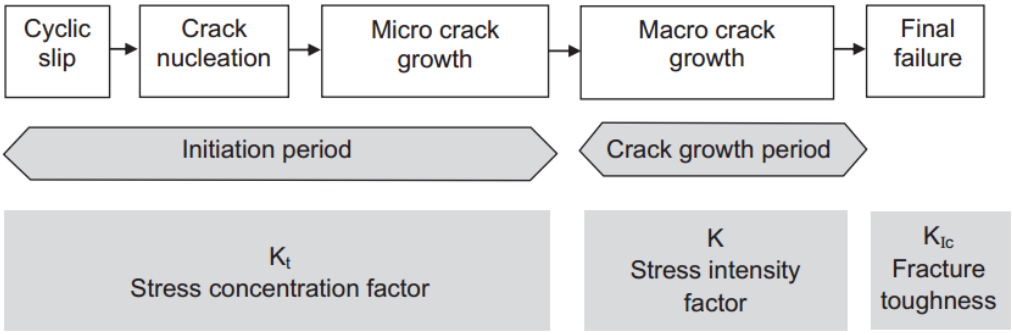

Figure 1. Phases of fatigue and process describing factors. **(Schijve & Yarema 2003)**

It was noticed in very early days of fatigue failure investigations that the crack nucleation on the surface of material is caused by material slip bands. Typical nucleation sites include also inter-material and surface defects. The time to nucleation of crack is called initiation period. After crack initiation, there are two more steps into which the crack growth can be separated. Next state of fracture is growth period during which the crack is growing steadily. Final failure occurs when the crack has weakened the structure enough for it to carry the load and the crack rapidly propagates through the structure which is the last step. These steps are often called Stage I, Stage II and Stage III respectfully.

The foundation for fatigue calculations has been said to be laid in between period of 1920-45. Great efforts were given especially by famous engineers such as Wöhler, Palmgren, Gassner and Griffith. However the very first known work in the field of fatigue dates back to year 1837 when Albert published his results on fatigue of conveyer chains at a mine in Germany. (Schütz 1996)

After the work by Albert another famous German engineer Wöhler, who is known for his famous Wöhler curve, began his work among fatigue life by measuring stresses and strains on railway car axles. Failures of train axles had grown into major issue in Germany and England in the 19th century. After developing various fatigue testing devices and contributing tests with notched and un-notched specimens he finally contributed his final work in field of fatigue in the end of 19th century. These results are these day known as

Wöhler's laws. It was Wöhler who proposed that material can fail under loads that are below static strength. (Schütz 1996) (Schijve & Yarema 2003)

In the era of 1920-45 significant findings on fatigue were made. Gassner started his work on theory of cumulative fatigue under variable amplitude loading which was further studied by Palmgren, Langer, Serensen and Miner. The linear cumulative fatigue damage law for variable amplitude loads is known these days as Palmgren-Miner rule (Hobbacher 2016). In the same era Föppl and Thum investigated methods to improve fatigue life by compressive residual stresses. It was also in this era when the foundation for fracture mechanics based fatigue analysis was laid by Griffith in 1920.

Variable amplitude fatigue life method, extensively investigated and developed by Gassner, has become widely accepted in the industry. The process of variable amplitude fatigue testing of real life component has remained essentially the same from the days of Gassner. Improvements were made in order to present the real life fatigue load conditions by Japanese Matsuishi and Endo who developed and published rainflow method for load spectra cycle counting from measured stress data. (Matsuishi & Endo 1968)

Originally Gassners work proposed use of blocked loading cycles. This theory could not be tested until 1960's due to the lack of proper testing devices suitable for running real random sequence load cycles. After the development of servo-hydraulic testing devises for example NASA and Schijve et al. from NLR tested the theory and noticed that blocked test cycle gave higher fatigue life compared to random sequence fatigue tests. Full scale simulations using electrohydraulic test devices became more common in the last decade of 20^{th} century and were performed for various structures.

Extensive research on fatigue of metals has resulted into great knowledge of different parameters affecting on fatigue life of structures. Many of these have been proven with physical tests but quantitative descriptions don't exist. It is safe to say that current knowledge lets us design against fatigue, despite the fact that fatigue life cannot be determined quantitatively. Due to these facts current recommendations for cumulative damage fatigue analysis are very variegated. Many methods have been developed and tested for various applications but they all fail to describe the fatigue of metals in general form. This sets engineer in role where the choice between different methods has to be made according to thorough evaluation of the conditions of the application.

2.1 Weld fatigue

Welded structures are notoriously difficult in terms of fatigue life assessment. Welding as a process causes significant changes into the material properties. It causes residual stresses that can be magnitude of yield strength of parent material. Weld bead is also usually a major discontinuity in the structure, causing high stress concentrations. Weld joints also include impurities that work as a crack nucleation sites increasing probability of crack initiation. Welded structures are assumed to include crack like defects thereby significantly reducing time spent on crack nucleation state of the fatigue life. (Chapetti & Jaureguizahar 2011)

Traditional fatigue analysis methods are based on S-N curves that are derived from fatigue test performed on sample pieces. This data is typically presented in terms of nominal stress for the specific sample. Using S-N curves has some limitations that can be addressed with the use of so called local approaches for fatigue calculation. Limitations arise from the differences on welds used for determining S-N curve and that to be manufactured. Main differences are weld geometry, welding method, material and defects that are not typically clearly specified or comparable between test sample and manufactured piece. The S-N curves also don't describe the progress of the fatigue. To be able to asses these limitations, many local approaches have been developed. (Radaj et al. 2006)

For welded structures typical fatigue analysis is based on FAT-classes. FAT-class is based on assumption of maximum acceptable stress level for defined weld detail to give fatigue life of 2E6 cycles. These values are determined by fatigue testing of sample pieces on fatigue test rig.

To be able to choose the right FAT-class for the application, the properties of the weld needs to be known with very high detail starting from weld type. Other information that needs to be included are welding process, post processing and load conditions. Even the environmental conditions for which the weld is subjected to must be considered. When the structure is subject to variable amplitude loading the cut of the load-time history, Rainflow matrix, load ratio, irregularity factor and the maximum peak value should also be known to choose correct FAT-class. (Sonsino 2007)

It is easy to understand that due to so many different variables and usually unknown factors this method suffers from lack of generality. Immense amount of fatigue test would be needed to cover even the most general operating conditions while still leaving lot to be guessed by engineer in order to derive the fatigue life.

Due to very complex conditions analytical method for fatigue life calculations has not been found. The methods that have been implemented usually require extensive testing and data collecting. Complex geometries cause that analytical stress state evaluation is hard or impossible to perform, therefore finite element analysis (FEA) is widely utilized

to determine the stresses. When the stresses present in weld are determined, fatigue life calculations can be carried out.

Most common methods for fatigue life determination are discussed in following sections. The methods presented are widely used by industry and have been validated by empirical tests by many researchers. Results from different papers were collected into single book by Radaj et al. in 2006 (Radaj et al. 2006).

Nonetheless all these methods have their limitations and problems which will be presented. Choosing the correct method for accurate fatigue life determination has to be done carefully. Depending on the type of weld joint, materials and load condition different methods and table values for fatigue life estimation has been established.

3. FATIGUE ANALYSIS

There are great number of different fatigue analysis processes. Different processes have been described by many researchers over past decades for different applications. For variable amplitude stresses these theories have been developed since 1920's. Three main steps can be identified in most of the fatigue analysis theories.

Most of the theories include cycle counting, fatigue stress determination and damage calculation. Various methods for each step have been developed and different combinations of these methods are used for fatigue life assessment. Most common methods are presented here to give overlook of the available methods that are included in the fatigue life theories.

3.1 Cycle counting

Most of the structures in practical life are loaded by variable amplitude (VA) loads. In some applications the typical loads are variable amplitude, multiaxial and non-proportional. This type of complex load condition makes stress cycle determination difficult.

To perform any fatigue calculations, it is absolute necessity to first determine the actual load-time history (Sonsino 2007). To determine the stresses that act in the structure during operation, field tests in operating conditions are required. Measurements are usually done by placing strain gauges to locations that are known to be critical for fatigue life. Strain data is collected using data acquisition device.

After measurement the test data can be post processed to identify the fatigue loading cycles. For this purpose several cycle counting algorithms have been developed (Marsh et al. 2016). Some of the accepted and most common cycle counting algorithms for variable amplitude stress data are presented here.

3.1.1 Rainflow counting

Rainflow counting method was originally proposed by Japanese Matsuishi and Endo. In their paper the cycle identification was assimilated to rainflow down traditional Japanese pagoda roof. It is likely the most common method that is used currently for cycle counting.

The novel method can be visualized by rotating peak-valley filtered stress-time signal plot 90 degrees.

Rainflow cycle counting can now be done by creating streams starting from every inner corner (peaks and valleys) of the rotated stress time chart. One half cycle is calculated every time when a stream falls of the edge and ends into the end of time history (A1, A4 and B4) or when the stream merges into a stream that started earlier (B2 and A3) or when stream merges into any stream that has greater magnitude (B3 and A6).

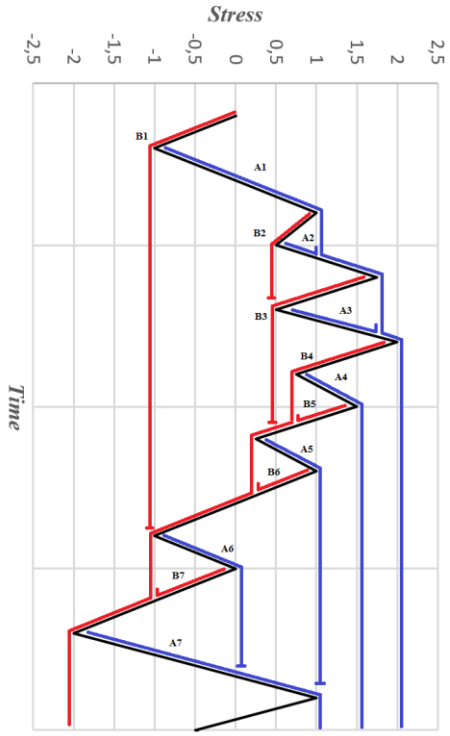

Figure 2. Visualization of rainflow cycle counting method performed to peak-valley reduced stress-time data.

The half cycles are collected into table and the ranges are combined to calculate amount of full cycles in the spectra. Half cycles are simply calculated to define amount of cycles in the spectrum.

Table 1. Rainflow ranges of example stress data.

	From	To	Range		From	To	Range
B1	0	-1	1	A1	-1	2	3
B2	1	0,5	0,5	A2	0,5	1	0,5
B3	1,75	0,5	1,25	A3	0,5	1,75	1,25
B4	2	-2	4	A4	0,75	1,5	0,75
B5	1,5	0,75	0,75	A5	0,25	1	0,75
B6	1	0,25	0,75	A6	-1	0	1
B7	0	-1	1	A7	-2	1	3

Table 2. Rainflow cycle count table of example stress data

Range	Count
4	0,5
3	1
1,25	1
1	1,5
0,75	2
0,5	1

In real life measurements the stress levels can have virtually infinite amount of different values which would result into unpractical amount of stress levels. To reduce the amount of stress levels it is necessary to decide a stress threshold in which the different stress levels are reduced into one stress level.

Different algorithms have been developed for computerized Rainflow cycle counting. Some of the algorithms are capable of counting the cycles during the stress measurements before the entire time history is known. The algorithms that are used to perform Rainflow cycle counting are not discussed here in more details. For detailed view of some Rainflow algorithms one can familiarize oneself with article by Downing and Socie. (Downing & Socie 1982)

Latest software for stress data processing provide histogram presentation of the rainflow cycle counting (Figure 3). This graph can be used to visualize the scatter of stresses in the load-time history.

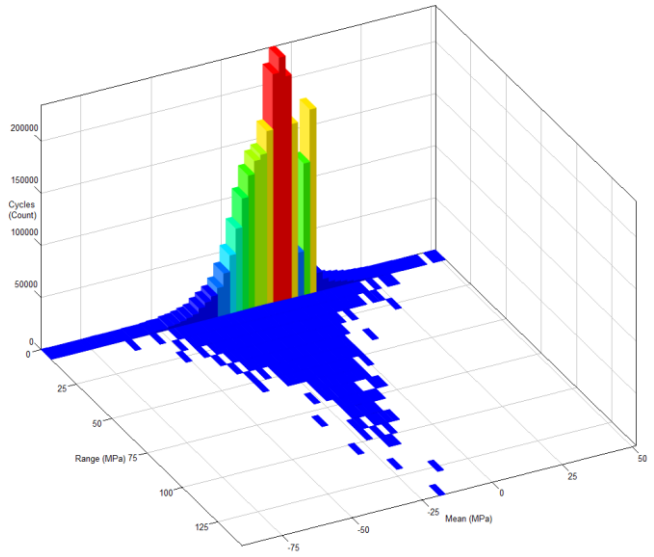

Figure 3. Histogram presentation of rainflow cycle count made with nCode Design-Life software.

3.1.2 Other methods

ASTM E 1049-85 standard lists some of the cycle counting methods that are acceptable in variable amplitude fatigue analysis. Overview of the basic forms of these methods are presented with example stress-time signal. (ASTM E 1049-85 Standard practices for cycle counting in fatigue analysis, in: 1997)

Level crossing method is a method where stress-time data is processed so that stress count is recorded every time the load exceeds certain level above or below reference load (Figure 4). These counts are then paired to form full cycles.

One method for cycle reconstruction is to first combine the two extreme values to form the most damaging cycle. Next the second most damaging cycle is formed and this process is repeated until all the counts are paired. Stress reversal is assumed to occur in halfway of the cycle.

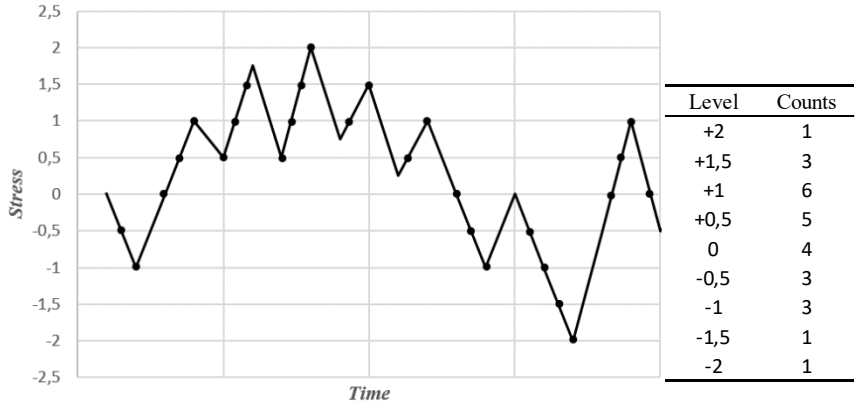

Level	Counts
+2	1
+1,5	3
+1	6
+0,5	5
0	4
-0,5	3
-1	3
-1,5	1
-2	1

Figure 4. Level-crossing cycle counting method.

Some modifications of level-crossing method has been proposed, like restricted method where on tensile side only increasing levels are counted and similarly on compressive side.

Peak-Valley cycle count method identifies peaks and valleys that occur above and below certain reference level. These counts are then paired in similar manner as the counts in level-crossing method. Small variations in the stress-time data are often filtered to reduce the amount of peaks and valleys. This can be done by mean-crossing peak counting. This method counts only the largest and smallest peaks between two suggestive time points.

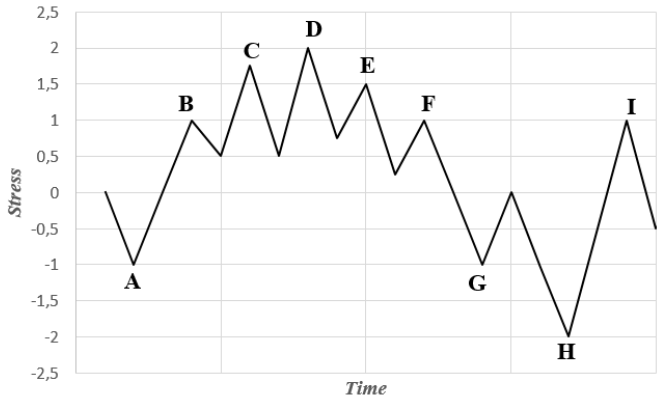

Peak	Counts
+2	1
+1,75	1
+1,5	1
+1	3
-1	2
-2	1

Figure 5. Peak-valley cycle counting method.

Range-pair counting is recognized as Rainflow related method where range counts are taken as cycles if there exists a subsequent pair in opposite direction. The rules for this method are listed in ASTM E 1049-85 standard in more details. Each peak and valley is counted only as half cycle and if there exist a pair it forms full cycle

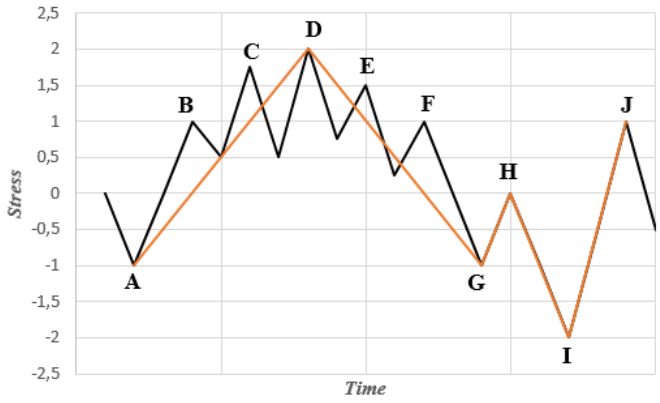

Peak	Counts	Range	Cycle count
+2	0,5	4	1, D-I
+1	0,5	3	0
0	0,5	2	1, A-J
-1	1	1	1, G-H
-2	0,5		

Figure 6. Range pair fatigue cycle counting method.

3.2 Fatigue stress

To be able to assess the fatigue life of a structure one needs to choose the appropriate method for determining the stress that is driving the fatigue. Various different methods have been proposed for determining the stress at the proximity of the weld or a structural discontinuity. Different methods for defining the stress at weld contour has been created but due to increase in computing power FEA based methods have become the industry standard. Other methods are based on parametric formulae or tables. (Hobbacher 2016)

Most common methods used these days are presented in following sections. This will help to understand the current state of stress evaluation at most critical areas of weld joints. The methods presented here are applicable for FEA based fatigue analysis.

3.2.1 Hot spot

Hot spot stress method combines all the stress raising effects of the structural detail into single formula. Structural hot spot stress is specified by extrapolating FEA analyzed or measured stresses at proximity of weld to the weld toe. Extrapolation is applied to places where the fracture is expected to occur. The locations where the hot spot stress calculation should be performed can be determined by using FEA calculations to find areas of high stress ranges under operation conditions or by previous experience on the possible fracture initiation locations. (Hobbacher 2016)

Hot spots are divided into two types (*a* and *b*) depending on their location and orientation on the plate in respect to the weld toe. Type *a* hotspots include weld toes on plate surfaces whereas type *b* hotspots consist of weld toes at plate edge.

For hot spot stress determination by FEA some special attention has to be given for meshing. It is advisable to model also the weld seam to avoid underestimation of the stiffening effect of the weld seam.

For type *a* hot spots the stresses are extrapolated by following formulas:

$$\sigma_{hs} = 1.67 * \sigma_{0.4t} - 0.67 * \sigma_{1.0t} \quad (1)$$

$$\sigma_{hs} = 2.52 * \sigma_{0.4t} - 2.24 * \sigma_{0.9t} + 0.72 * \sigma_{1.4t} \quad (2)$$

$$\sigma_{hs} = 1.50 * \sigma_{0.5t} - 0.50 * \sigma_{1.5t}, \quad (3)$$

where t in subscript is plate thickness and $\sigma_{0.4t}$ is stress derived from FEA results in distance of 0.4*t times plate thickness respectively. Equation (1) extrapolates the stress from reference points to weld toe. For this formula element size must not exceed 0.4t. Equation (2) gives quadratic extrapolation of the stress. This formula is especially recommended to be used in cases where apparent non-linear behavior is present in the proximity of weld. It is also recommended in case of thick-walled structures. In case the model was meshed with higher order elements with element size higher or equal to plate thickness, equation (3) should be used. For this equation the stresses must be derived from mid-side nodes on the FEA results.

For type b hot spot stresses following formulas shall be applied:

$$\sigma_{hs} = 3 * \sigma_{4mm} - 3 * \sigma_{8mm} + \sigma_{12mm} \quad (4)$$

$$\sigma_{hs} = 1.5 * \sigma_{5mm} - 0.5 * \sigma_{15mm} \quad (5)$$

For type b hot spot stress the plate thickness doesn't affect the stress distribution. Thus in equations (4) and (5) have the distances given in millimeters rather than relative distance as function of plate thickness.

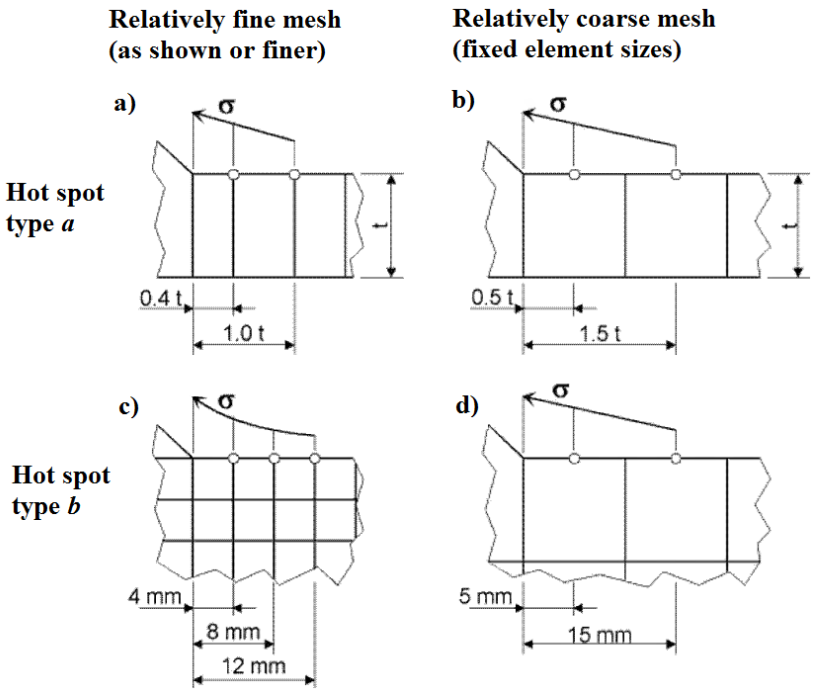

Figure 7. Illustration of stress extraction points in welded structures. Figures a) and b) for type a hot spot and c) and d) for type b hotspot.

Hot spot stress method can also be combined with experimental strain gauge measurement. In experimental methods the gauges are placed on the surface of the structure in the proximity of the weld. Amount of gauges and their locations are dependent on wall thicknesses and the type of structure.

For defining type *a* hot spot strain from measured data, following equations have been derived:

$$\varepsilon_{hs} = 1.67 * \varepsilon_{0.4t} - 0.67 * \varepsilon_{1.0t} \quad (6)$$

$$\varepsilon_{hs} = 2.52 * \varepsilon_{0.4t} - 2.24 * \varepsilon_{0.9t} + 0.72 * \varepsilon_{1.4t} \quad (7)$$

and for type *b* hot spot strain:

$$\varepsilon_{hs} = 3 * \varepsilon_{4mm} - 3 * \varepsilon_{8mm} + \varepsilon_{12mm} \quad (8)$$

Where ε_{hs} is the hot spot strain, $\varepsilon_{0.4t}$ is measured strain 0.4*t distance from the weld toe. The indices describe the distances from weld toe respectively. The distances of the gauges from weld toe are defined in each formula depending on method. It is recommended that in case of thick plates the center point of first gauge is at distance of 0.4t from the weld toe. However this might not be possible in case of thin plates. In such case it is recommended to be placed so that the leading edge of the gauge is at distance of 0.3t from the weld toe.

After the measured strain values have been extrapolated to weld toe it can be further transformed into stress. In case of uniaxial stress state the strain is simply transformed into stress according to Hooke's law (9) of linear elasticity. If biaxial stresses are present, rosette type strain gauges should be used. In that case the stress is derived with equation (10).

$$\sigma_{hs} = E * \varepsilon \tag{9}$$

$$\sigma_{hs} = E * \varepsilon_x * \frac{1 + \nu * \frac{\varepsilon_y}{\varepsilon_x}}{1 - \nu^2}. \tag{10}$$

When hot spot method is used to determine the stress, FAT values need to be corrected by thickness correction factor. The thickness correction is recommended by IIW and Eurocode. Reference thickness in IIW documents is 25 mm and the correction is applicable to structures thicker than that.

3.2.2 Effective notch stress

Effective notch stress (ENS) method for fatigue life assessment of weld joints is based on evaluating of the total stress at modeled weld contour. The method was originally proposed by Sonsino et al. He derived the method for both thin and thick plates. Theory for thick plates originates from hypothesis of micro-support by Neuber (Sonsino et al. 2012) (Radaj et al. 2013).

To be able to define the stress at weld contour with FEA one must model the weld geometry accurately. On the concept of ENS the weld geometry and fictitious rounding at weld toe or root is modeled to simulate the stress concentration at the vicinity of the weld (Figure 8). (Hobbacher 2016)

The critical factor in ENS is the radius on the edge of the weld toe. IIW recommendations currently propose 30 degree weld angle for butt welds with 1 mm radius at weld toe and root. Other radii has been proposed in literature for different applications. Originally when ENS method was represented by Sonsino et al. they proposed use of two different radiuses. For thin plates ($t < 5$ mm) they proposed value of 0.05 mm and for plates thicker than that 1 mm. Since then some researchers have found radius of 0.3 mm to correlate better with fatigue tests. Schijve in his paper questions the use of fixed radiuses and proposes use of continuous radius range. He proposes that the radius should be defined as function of the weld height. (Schijve 2012) For weld geometry modelling the actual as-welded geometry can be used in case that it is known.

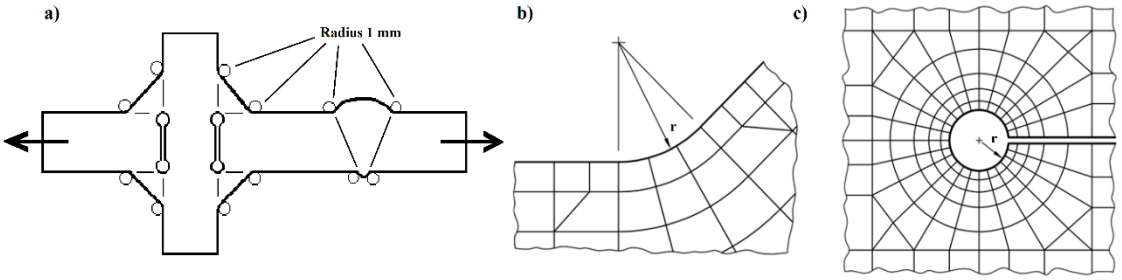

Figure 8. Cross sectional figures of weld joints with fictitious notches at weld toe and root. a) Fillet and butt weld b) Example of element mesh at weld toe or root c) Example of element mesh at root of fillet weld **(Stenberg et al. 2015)**

For FEA simulation IIW recommends the use of elements that are in maximum ¼ size of the radius to be used to model the weld contours. In case of 1 mm radius, the element size would be in maximum 0.25 mm when higher order elements are used (Figure 8b).

After the notch is modeled in FEA the structure is loaded with actual loads and the stress value at the weld geometry is then extracted from FEA results. The results are then compared to FAT values given for example in IIW recommendations. IIW recommends for butt welds FAT 225 for constant amplitude stresses. However Pedersen et al. noticed in their paper that with effective notch stress method some of the specimens extracted from literature fell on conservative side. Thereby they propose the use of FAT 200 for butt welds. (Pedersen et al. 2010) In variable amplitude loads the FAT value is lowered significantly. The current recommendation for FAT value at variable amplitude loading is 71.

Butt welds are also extremely sensitive for misalignment and IIW recommends correction factor of 1.1 for but welds welded at shop conditions.

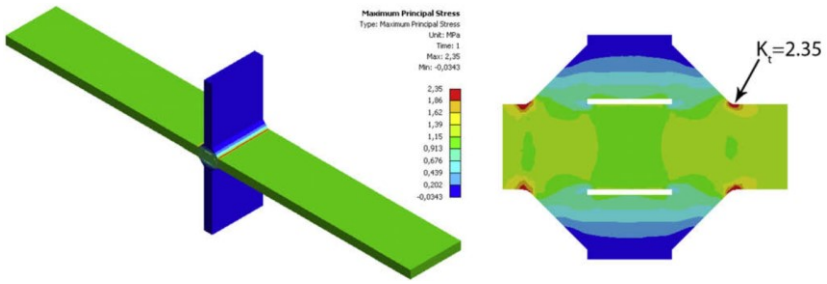

Figure 9. Stress concentration factor in cruciform fillet welded specimen under unit load. **(Pedersen et al. 2010)**

Using ENS method with variable amplitude load can be done by regenerating the worst measured strain state of the object by FEA and reading the stress at FEA model in the proposed fatigue failure location. Simulated stress at weld toe is then compared to the maximum peak stress of the measured load spectra. The spectra can be then scaled to

match the analyzed ENS and measured maximum peak stress. After that fatigue life can be calculated using the method of choice.

3.3 Fatigue life calculation in variable amplitude loading

For fatigue life calculation it is crucial to understand the requirements of the application. Designer needs to understand the consequences of possible failure and how to prevent them. Depending on the requirements of the application different fatigue design strategies should be used. Four different strategies has been listed by Hobbacher in IIW recommendations.

Infinite life design is recommended to be used on components that are not to be inspected or monitored during usage and are loaded by CA or near CA loads. *Safe life* design gives very high survival probability and it is to be used in structures where regular inspections are not possible and possible failure would have very high consequences. *Fail safe* design is based on assumption that the structure can withstand extensive fatigue cracking without failing. This is typically achieved by hyper-static structure. With fail safe method regular monitoring is not necessary as failures can be detected after occurrence and repaired without ultimate failure. *Damage tolerant* design is based on assumption where cracks are allowed to be formed during use but they are detectable before total failure. This method necessitates regular inspections. (Hobbacher 2016)

According to old belief there exists limit after which structure newer fails. However recent papers questions existence of infinite life for structures, especially welded ones. In this paper our goal is to design the boom for damage tolerant design, with finite fatigue life.

Two main approaches for fatigue life assessment at present are SN-curve based method and fracture mechanics based method. In here we are going to give insight of fatigue life assessment methods based on both approaches.

3.3.1 Palmgren-Miner rule

Palmgren-Miner rule is a method used in variable amplitude fatigue life analysis. Palmgren-Miner rule is based on S-N curves and assumption of cumulative fatigue damage. It assumes that all stress ranges present in structure damage it. The damage with each stress level is derived from S-N curve and finally damage of all cycles in the measured stress spectrum are summed together resulting in total effect, hence name damage sum.

Originally Palmgren-Miner rule assumed damage sum of one to represent fatigue failure, but recent studies have shown that for welded structures the values can be between 0.1-10 at failure. (Hobbacher 2016) These findings have aroused need for modifications to Palmgren-Miner rule.

The original presentation of Palmgren-Miner rule describes the damage sum of one spectrum in uniaxial loading,

$$D_{spec} = \sum_{1}^{i} \frac{n_i}{N_i} \leq D_{specified} \tag{11}$$

In which n_i is the amount of cycles of one stress level i in the rainflow spectra and N_i is the fatigue tolerance of the structure against the stress level. The fatigue tolerance is derived from structure corresponding SN-curve (Figure 10). $D_{specified}$ is maximum value of damage sum that the structure is assumed to withstand. If the damage sum of the spectrum is smaller or equal to $D_{specified}$ the structure will not fail. It is also simple to calculate how many hours of spectral load the structure would hold by dividing specified damage sum by damage sum of one spectra and multiplying the result with the length of the spectra in hours.

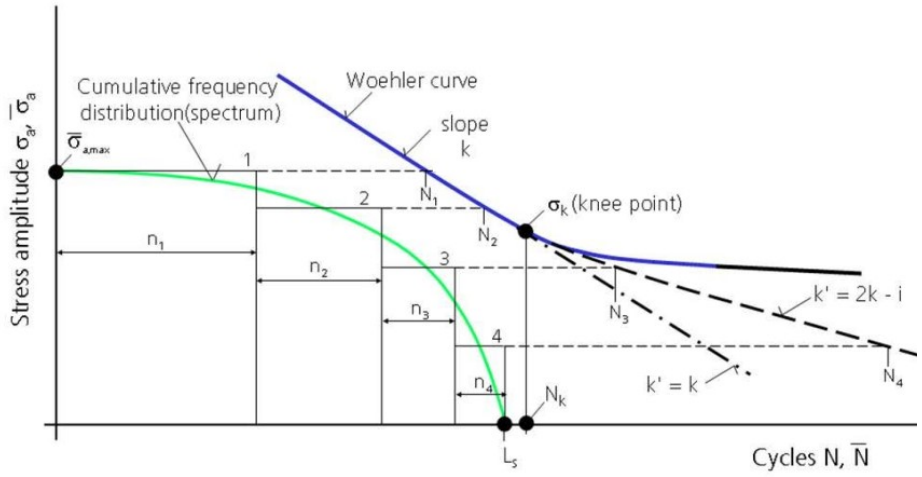

Figure 10. Cumulative fatigue damage calculation from extended S-N (Wöhler)-curve according to Palmgren-Miner rule. Extension made according to proposal by Haibach.

Originally Miner assumed that stresses below certain level could be neglected in damage sum. Haibach proposed modification on SN-curves to improve the accuracy of Palmgren-Miner rule. His modification propose reduction in the slope angle of SN-curve after 2E6 cycles (Figure 1).

$$k' = 2 * k - m \tag{12}$$

Where k' is the slope angle after 2 million cycles, k the original slope and m is the material and case dependent reduction constant. For forged or rolled components value reduction constant of 1 is proposed and for welded and cast components value of 2. With extended S-N-curve the damage effect of smaller stresses can be calculated and taken into

account in damage sum. The extension is based on findings that also the lower stresses together with higher amplitudes have damaging effect on structure, although not as significant as higher stresses.

For multiaxial load cases IIW recommendations suggest method of equivalent stress. Based on a modification of Palmgren-Miner rule for determining equivalent stress from variable amplitude loading

$$\Delta\sigma_{\mathrm{a,eq}} = \sqrt[m_1]{\frac{1}{D_{spec}} * \frac{\sum\left(n_i * \Delta\sigma_{i,S,d}^{m_1}\right) + \Delta\sigma_{L,d}^{(m_1-m_2)} * \sum\left(n_j * \Delta\sigma_{j,S,d}^{m_2}\right)}{\sum n_i + \sum n_j}} \qquad (13)$$

where D_{spec} is the corresponding Miner sum, $\Delta\sigma_{\mathrm{a,eq}}$ equivalent stress range, m_1 and m_2 slopes above and below knee point on the SN curve respectively. $\Delta\sigma_{i,S,d}$ and $\Delta\sigma_{j,S,d}$ are the design values of stress ranges above and below knee point and $\Delta\sigma_{L,d}$ stress range at knee point on the SN curve. n_i and n_j are number of cycles applied at stress ranges above and below the knee point. Same formula is used for equivalent shear stress respectively.

After determining the equivalent stresses from rainflow spectrum with equation (13) it can be substituted into modified Gough-Pollard equation

$$\left(\frac{\Delta\sigma_{a,eq}}{\Delta\sigma_{a,SN}(N)}\right)^2 + \left(\frac{\Delta\tau_{\mathrm{a,eq}}}{\Delta\tau_{a,SN}(N)}\right)^2 \leq D_{specified} \qquad (14)$$

where $\Delta\sigma_{a,SN}(N)$ and $\Delta\tau_{a,SN}(N)$ are the fatigue stress limits with N cycles under pure tension and torsion respectively. $D_{specified}$ is threshold value determined by fatigue testing or by recommendations in literature. These values typically vary between 1 – 0.5 depending on load condition. IIW recommendations propose value of 0.5 for variable amplitude non-proportional load spectra.

Other methods for combining shear and normal stresses have been proposed by many authors. Those methods and their validity in fatigue analysis was presented and extensively investigated by Ninic and Stark. (Ninic & Stark 2007) The Gough-Pollard method presented here is the current recommendation by IIW for ductile and semi-ductile materials.

3.3.2 Critical plane method

Many of the methods for multiaxial stress fatigue are based on determining equivalent stress acting on critical plane where fatigue failure is suspected to occur. Various criteria have been developed to address multiaxial variable amplitude fatigue problems but in literature the critical plane method is dealt most.

Carpinteri et al. proposed in their paper a modification to original critical plane method to deal with problems of multiaxial, variable amplitude random loading. (Carpinteri et al. 2003) Their formulation is based on a method of nonlinear combination of shear and normal stresses acting on critical plane to form equivalent stress.

In case of multiaxial random loading a single critical plane can't be defined. Carpinteri et al. propose an averaging method for finding critical plane Δ. Critical plane for each time point in normal stress data is determined. Critical plane is then found by averaging individual critical planes resulting in mean critical plane.

Time dependent stress data is split into shorter sections with length of z – points. The subcycles are deduced into peak-valley data. Equivalent stress is then formed from the peak-valley data. This equivalent stress data is then used in similar manner as in Palmgren-Miner rule to calculate the fatigue damage.

3.3.3 Fracture mechanics

One of the methods that can be used for fatigue life assessment is fracture mechanics. It has not been widely utilized in industry due to its mathematical complexity. Modern FEA software include fracture mechanics extended analysis which can be used to predict fatigue life and crack propagation direction in structures. Two main fracture mechanics based approaches are Linear Elastic Fracture Mechanics (LEFM) and Elastic Plastic Fracture Mechanics (EPFM). (Hobbacher 2016)

Three modes of fracture opening has been recognized. Each mode is characterized by the force that is opening (driving) the crack. In Mode I the crack is subjected to tensile stress collinear to crack surface. Mode II is driven by in plane shear stress and Mode III by out of plane shear stress. (Figure 11)

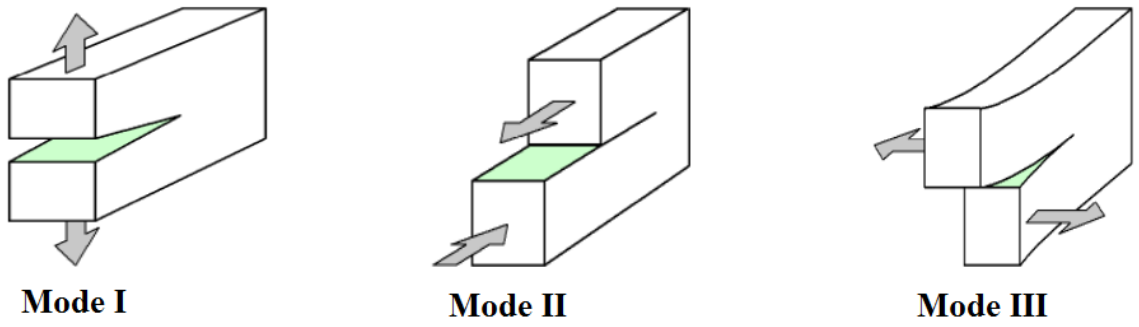

Figure 11. Fracture crack opening modes.

It has been shown that there are at least seven factors affecting the crack growth under non-proportional mixed-mode loading. All of those factors aren't currently fully understood thus meaning that theoretical support for the current formulations is thin. Due to many unknown factors many conservative assumptions must be made. In fracture mechanics based approach it is assumed that cracks are present in weld seam after welding process. This means that time to crack initiation is negligible in terms of fatigue life (Krasovskyy & Virta 2014) (Hobbacher 2016). This assumption simplifies the calculations.

For sake of simplicity in this thesis we will be focusing on LEFM. Theory of linear elastic fracture is applicable for materials with low toughness thus being suitable for high strength steels. The initial assumption in LEFM is that the material is isotropic and linear elastic. Main parameter in LEFM is stress intensity factor K_I that acts as a loading parameter at crack tip. Crack is proposed to start propagate after the stress intensity factor exceeds the material specific critical value, fracture toughness K_{Ic}.

Fracture toughness is determined by appropriate tests. Standardized test methods are given by e.g. ASTM-Standard E399-90. However it has to be noted that fracture toughness is strongly influenced by factors such as microstructure, heat treatments, environmental conditions, loading history and temperature. Thereby conservative assumptions are needed unless the conditions are stable and well known. (Gross & Seelig 2011)

K-factor based estimation of fatigue life has some limitations. The method is no longer valid when K_{max} values are high and instead it is proposed that J-integral based approach may be more appropriate. (Anderson 2005) Another limitation is subject to the well-known Paris' law. The law is based on similitude assumption which states that crack growth can be described by single parameter derived in initial condition of the structure. Similitude can be assumed when cyclic loads with high R ratios are present. This is due to crack closure effect which has shown to significantly retard the crack propagation with low stress levels. In welded structure there are high tensile residual stresses at weld area. Due to this effect similitude is valid assumption for cracks at weld joints. (Anderson 2005)

Stress intensity factor is depending on cofactors such as crack location, crack shape and body geometry. There are multiple methods for determining the stress intensity factor. For certain types of cracks this can be derived analytically (for example through thickness crack in infinite plane). Typically some assumptions have to be made to determine the stress intensity of the structure of interest. The solutions and methods for finding stress intensity factors won't be explained here.

Gross and Seeling have given detailed examples of various methods for calculating stress intensity factors for different conditions. For practical engineer K_I values have been provided in literature. The stress intensity factor can also be derived by FEA software such as Ansys. Factors for some common structural details and load conditions have been listed

in IIW recommendation for welded structures. Some analytical stress intensity factors have been derived also by Gross & Seeling in their book. (Gross & Seelig 2011)

If similitude can be assumed then fatigue life assessment can be performed using fracture mechanics approach and K-factor. Fatigue life can be obtained by integrating the crack from initial size of a to acceptable maximum size of a_i. Basic formulation for fatigue crack propagation is Paris power law for crack propagation,

$$\frac{da}{dN} = C_0 * \Delta K_I^m \; if \; \Delta K < \Delta K_{Ic} \; then \; \frac{da}{dN} = 0, \tag{15}$$

where C_0 is constant of the power law, ΔK_I is the range of cyclic load stress intensity factor, m exponent of the power law and N number of cycles. Paris power law states that crack won't propagate if the stress intensity factor is below fracture toughness.

Paris power law can also be used for variable amplitude load cases by calculating the crack propagation for each stress level in spectrum separately and summing them to derive crack propagation for one complete stress-time history. When the length of one load spectra and required life time is known it is possible to calculate how many cycles the structure should last. Then number of time histories for maximum crack size can be easily calculated by,

$$N_p = \int_a^{a_i} \frac{da}{C[\Delta K]^m} = \int_a^{a_i} \frac{da}{C\left[F(a)\Delta\sigma\sqrt{\pi a}\right]^m} \tag{16}$$

where $F(a)$ is correction factor for stress intensity factor. If the N_p is smaller than the required number of cycles, the structure will fulfill the lifetime requirement. The formulation above is applicable for single mode fracture. In case of mixed mode fracture a generalized fracture criterion must be formulated and used instead.

In fracture mechanics based approach many correction factors are used to address the uncertainties in the calculation. Corrections are made due to e.g. geometric conditions, environmental conditions and weld conditions.

Sometimes it is necessary to determine the critical crack length,

$$\sigma_f = \frac{K_{Ic}}{\alpha\sqrt{\pi a_i}}, \tag{17}$$

where σ_f is the failure stress and α is a geometrical parameter. By solving the equation for a_i and substituting maximum peak stress into failure stress the critical crack length can be determined. Critical crack length can be used as maximum crack length in (16) to determine cycles to failure. (Hobbacher 2016) (Gross & Seelig 2011)

For constant material parameters in Paris power law IIW recommendations gives characteristic values for steel, which can be used unless better information is available. If fatigue life is calculated with fracture mechanics it is recommended to verify the results by tests.

4. FATIGUE LIFE IMPROVEMENT

Welded structures in as-welded state are very prone to fatigue failures, and thus multiple different methods for improving fatigue properties of a weld has been developed. Typically welding results in very significant residual stresses at welded structure. It has been observed by multiple researchers that tensile residual stresses on the weld joint has significant effect on reducing fatigue strength of the welded structure (Sonsino 2009a). Another significant factor in fatigue life of weld is the weld geometry (Kirkhope et al. 1999). Thickness variation and sharp transition area between weld and base material have significant combined effect on reducing fatigue life of the structure.

Weld fatigue life improvement techniques are focused on improving or eliminating the features mentioned above. Most of them are post welding treatments which require extra labor and time after the welding process. In this section different methods for improving fatigue life of weld joints are discussed. However it must be stated that most of these methods focus on improving the features on weld toe and are not applicable to improving the fatigue properties on root side of the weld in certain structures. (Hobbacher 2016).

4.1 Weld shaping

During typical welding process molten metal is added onto a groove between base materials to form a joint between the parts to be connected. This added material (bead) causes local variation in the thickness of the plate, causing stress concentration at the toe and root of the bead. Geometrical changes together with typical weld impurities, residual stresses and weld flaws has significant effect on the fatigue life of a weld. The purpose of weld shaping is to reduce the stress gradient caused by structural discontinuity of a weld. (Hobbacher 2016)

Typically welds are shaped by grinder after welding. The transition from weld to base material is ground smoother or even flat to reduce stress concentration (Figure 12). Stress concentrations at weld joint area can be reduced also by joint geometry design. Shape and location of the weld seam can have significant effect on fatigue life.

The effect of weld joint toe angle on the fatigue strength of butt-weld has been investigated by Chapetti and Jaureguizahar. They published in their work results where the effect of angle was clearly shown. With angle of 115 degrees the fatigue limit started from less than 100 MPa ending to fatigue limit of nearly 300 MPa with flat ground butt-welds. (Chapetti & Jaureguizahar 2011) These values are examples achieved with test sample and must not be confused to FAT-values.

Figure 12. Butt joint ground flat. Ponsse Oyj

Changes in the material thickness cause stress concentration to the transition areas. This issue is present also where reinforcements has been added. Shaping the edges of reinforcement is used to reduce the stress concentration. Example of reinforcement plate has been shown in Figure 13. The tip of the plate has been chamfered to reduce the stiffness of the plate tip and thus the stress concentration effect.

Figure 13. Chamfered reinforcement plate with fillet weld. Seam toe TIG dressed. Ponsse Oyj

In but welds common weld geometry has backing bar (Figure 14). The backing bar helps the welding process by helping to control the molten steel. Backing bar has significant drawback, it causes significant thickness variation at the weld area resulting in stress concentration.

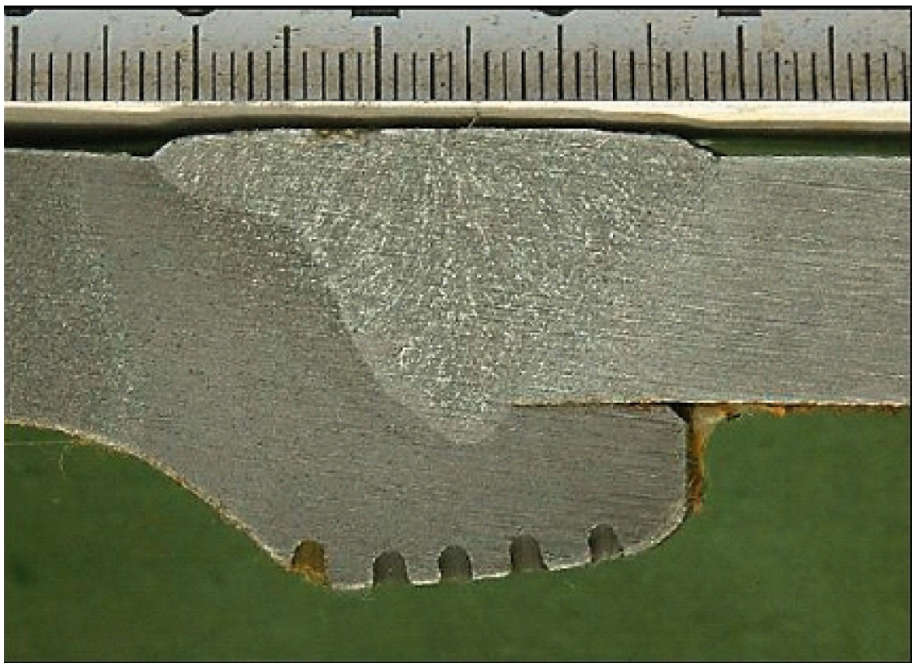

Figure 14. Butt weld joint with backing bar.

By visually observing the cross section of butt joint with backing bar, one can see the initial crack that is left into this type of structure after welding. Another significant drawback in backing bar is that it's also impossible to visually inspect the penetration of the weld. Modern welders make it possible to control the molten metal in butt welds without backing bar. This makes it possible to remove the backing bars from structures to improve the fatigue life off the joint.

4.2 LTT fillers

Welding process typically results into tensile stresses at weld root due to shrinkage of welding filler material and heat affected zone (HAZ). Low transformation temperature (LTT) fillers are welding consumables with alloying elements such as Cr and Ni. Due to the alloying additives these filler materials have low martensitic transformation temperature starting from 200 °C down to ambient temperature, which has been observed to reduce residual stresses significantly.

Body centered cubic (BCC) martensite is formed when fully austenitic steel goes through solid-state, displacive transformation as it is quickly quenched below martensite start temperature. Face centered cubic (FCC) austenite lattice has carbon atoms dissolved in its lattice. When the steel is quenched with very high cooling rate, the carbon atoms don't have time to diffuse out of the lath. Un-diffused carbon atoms in the martensite lath cause high level of dislocations. This process results in martensite. (Nishiyama 1978)

Welded structure is a key example of case where very fast cooling rates are present. Typical welded structures are massive and thus resulting in fast heat absorption to surrounding material. Cooling rates at weld can be as high as hundreds of degrees of Celsius per second as discovered by Yonemure et al.

Due to fast cooling rates martensitic transformation occurs in welded joints. In this process of phase transformation from austenite to martensite a very large volume change is present. Moyer et al. used dilatometric investigation to determine the volume expansion of Fe-C alloys during martensitic transformation. They found out that volumetric expansion could reach levels of 3.1 % with carbon percent of 1.01. (Moyer & Ansell 1975) The relation between carbon content and dislocation density was concluded by Morito et al. in their paper (Figure 15). They state out the relation between volume change and dislocation density. Interesting note in their work is the reduction in dislocation density after carbon content of 0.61 %. (Morito et al. 2003)

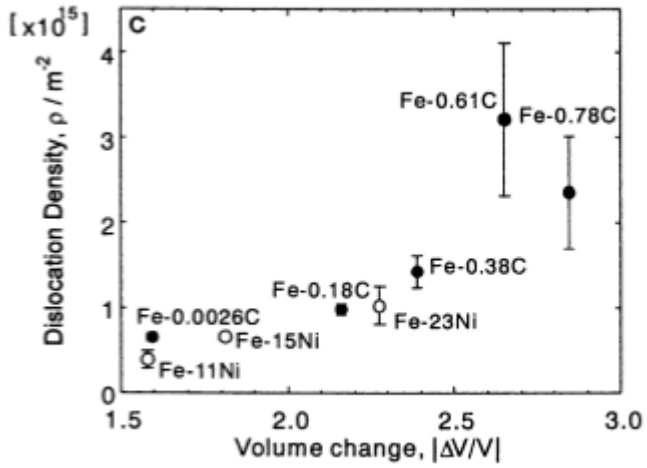

Figure 15. Correlation between volume change and dislocation density in different Fe-C and Fe-Ni alloys. (Morito et al. 2008)

Detailed process of phase transformations is not of our interest thus it is not discussed here more. For further reading Bhadeshia (Bhadeshia, H K D H 1999) and Nishiyama (Nishiyama 1978) has discussed this topic in their publications into fine details. Other phase transformation phenomena during welding process has been investigated by Yonemura et al. (Yonemura et al. 2006) by in-situ analysis during welding.

Martensite as a material is very hard (Bhadeshia, H K D H 1999) but it's not the martensite itself that results in improved fatigue resistance. Due to the expansion at the phase transformation process in low temperatures the toe of the weld is left even on compressive stress state, rather than high tension (Figure 16). The use of LTT fillers has been investigated extensively by many researchers like Ohta et al. They discovered in their studies that in certain specimen the fatigue limit could be doubled from 65 MPa to 130 MPa (Ohta et al. 1999). These results have been analyzed and concluded by Ooi et al. in their paper.

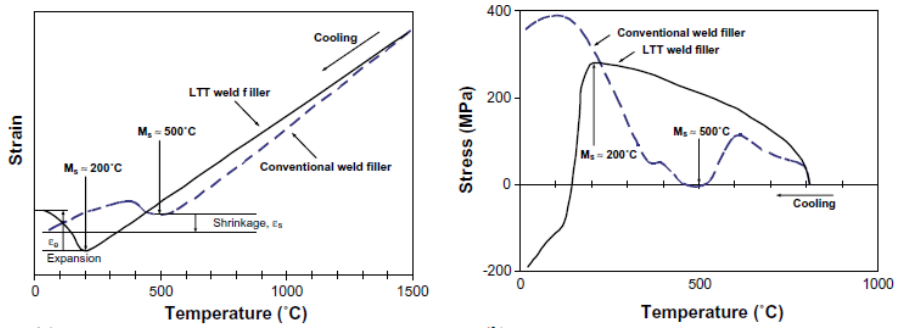

Figure 16. Stress and strain curves of welded structure during cooling with conventional filler and LTT filler material. **(Barsoum & Gustafsson 2009)**

LTT fillers have been proven themselves useful in practice by reducing or cancelling residual stresses at weld toe, both in transverse and longitudal direction of the weld. Reduction in residual stresses results also less weld zone distortion which is also beneficial.

It has been proven that LTT fillers improve fatigue resistance in all types of weld geometries. Harati et al. tested various different weld geometries including but weld and measured improvements up to 46 % in butt weld fatigue strength compared to IIW recommendation for FAT value with constant amplitude loading. (Harati et al. 2017)

Generally improvements up to 50% have been reported in mean fatigue strength with CA loading. However Barsoum and Gustafsson in their study proved that under variable amplitude loading with high mean stress improvements of only 12 % could be obtained. Some studies like one made by Bhatti et al. shows no improvement in fatigue life with VA loading at R = 0.5 (Bhatti et al. 2013) .This can be explained by relaxation of residual compressive stresses under high tensile stress amplitudes. They also state that improvement in fatigue life is better with higher cycles (lower stress). (Barsoum & Gustafsson 2009)

4.3 Residual stress modification methods

Residual stress methods concentrate on modifying local stress state in and around the areas where the crack propagation is most likely to initiate. In welded structures the most critical area is weld toe and root, where there is usually tensile residual stress and notch effect due to weld geometry.

Typical residual stress weld improvement methods are hammer peening (needle peening), and shot peening. Both of these methods are based on applying severe local force on weld toe in order to plastically deform the toe. Plastically deforming the weld area results into beneficial compressive residual stresses that are proven, with experimental and analytical methods, to improve fatigue life of welded structure. (Sonsino 2009b) (Webster & Ezeilo 2001) (Champoux et al. 1988) They also reshape the weld toe resulting in smoother transition between weld and parent material and thus decreasing notch effect.

Shot peening is method where typically steel balls are accelerated to high speed and hit against work piece. This method was patented already in 1870 by Tilgham. In his method sand that was used as peening material was accelerated by air or steam and shot against the structure. His method was further developed in 1920 – 1940's as it proved to have positive effect on fatigue, stress corrosion and corrosion fatigue properties.

Ultrasonic impact treatment (UIT) or needle peening method is developed in co-operation by Northern Scientific and Technological Fund in Russia and Paton Welding institute in Ukraine. The development of this method started in early 70's and has been since further developed by Russian scientist Statnikov E.S. The treatment is also called high frequency mechanical impact (HFMI) treatment.

Needle peening is method where special peening tool is used to perform the treatment (Figure 17). The tool consists of power unit and the hand held device with the needles. Needles are impacted against the work piece in ultrasonic frequencies. Depending on application there can be multiple needles and different diameters of needles.

Figure 17. HFMI tool and different needle heads with one or more needles. **(Yildirim et al. 2013)**

Fatigue resistance improvement with UIT is based on multiple factors. The method relieves tensile residual stresses, results in compressive stresses at area being treated, results in work hardening at the surface of the material and reduces stress concentration at weld toe by reshaping the toe area. (Trufiakov et al. 1995)

Suominen et al. conducted high frequency impact treatment (HFMI) on HSS test samples to prove the applicability of the concept on these materials. Residual stresses after treatment were measured by X-ray diffraction. Their work showed that the method is applicable also with HSS steels. (Suominen et al. 2013)

Fatigue tests have been conducted to HFMI treated samples proving the method effective in all weld geometries improving fatigue resistance. Roy et al. conducted testing for multiple different samples with various welding geometries. They found significant improvement in fatigue resistance in all instances. (Roy et al. 2003) Yildrim et al. extracted test data from hundreds of fatigue tests and concluded it in their study. They found FAT value

improvement of 89 % at butt welds compared to IIW recommendations. These specimens were loaded with axial load at R = 0.1. (Yildirim et al. 2013)

During past decades multiple different tools and techniques have been developed to perform residual stress based post treatment. For readers information some of those are briefly listed below. All the methods are derived from the work of Statnikov on UIT. In 2005 Bozdana et al. introduced Ultrasonic Burnishing. Another method was developed by Pyun called Ultrasonic Nanocrystalline Surface Modification. In Europe many industrial companies still use pneumatic tools such that developed by Schmucker and Gerster and Ummenhofer. The differences in techniques presented here are in the way that that the peening head is moved, what contact force, stroke and frequency they use. All these different methods and the terminology has been extensively explained by Schulze et al. in their article. (Schulze et al. 2016)

These residual stress methods have been noticed to improve fatigue life of welded structures only in cases where low mean stresses are present (Roy et al. 2003). Current recommendations by IIW sets threshold value of R = 0.4 for residual stress methods presented here to be effective (Hobbacher 2016).

4.4 TIG dressing

TIG dressing assigns to improve the geometry of the weld toe in order to reduce stress concentration. It also removes slag inclusions and weld undercuts, thus removing crack initiation points. It has been shown by Martinez et al. that TIG re-melting also decreases harmful tensile residual stresses at the surface of the welded specimen in root area. They reported decrease from 360 to 256 MPa in stress level at the surface of the welded specimen. They also noticed that the peak tensile stress sifted lower (further from weld toe) and increased from 556 to 699 MPa. (Martinez et al. 1999) As mentioned before, decrease in residual stress has been proven to have positive effect on fatigue life.

TIG-dressing has been proven to improve fatigue life also under variable amplitude loading, although the improvement is far less significant than when loaded with constant amplitude. Huo et al. made fatigue tests for welded samples with variable amplitude loading and reported 80 % increase in fatigue strength and 2.5-17 times increase in fatigue life compared to IIW recommendations. (Huo et al. 2005) Similar results were also obtained by Martinez et al. They observed that in TIG dressed welds the improvement in weld toe shape is the driving factor in improvement of fatigue life. (Martinez et al. 1999)

Unlike methods that are based on compressive residual stresses, TIG dressing is not suffering from relaxing effect of high mean stress cyclic loading. Therefore TIG dressing can be effectively used in structures subject to cyclic loads with high R-value. Example of TIG dressed weld joint is shown in Figure 18.

Figure 18. Tig dressed weld root. Ponsse Oyj

5. TOPOLOGY OPTIMIZATION

Topology optimization (TO) is a method in structural optimization. In this FEA based method the use of material in given design space is optimized in terms of maximizing the effectiveness of the material with respect to given objective i.e. stiffness and heat conduction. TO doesn't need any initial design for finding optimal structure, making it very powerful designing tool. In most general form of structural optimization TO can be used to determine optimal material distribution with given loads and boundary condition in order to maximize the stiffness of the structure. This is done by minimizing the inverse of stiffness, compliance, with given mass or mass fraction constraint.

Topology optimization is part of material distribution based structural optimization methods. According to definition, in topology optimization the genus of the structure is changed. Genus is defined in mathematics as maximum number of cuttings that can be made along closed curves without resulting in disconnected manifold. In other words genus is the number of "holes" in the structure. In Figure 19c the genus of structure goes from 0 to 5 and in Figure 19b the genus remains unchanged. The other material distribution methods are shape and sizing optimization (Figure 19).

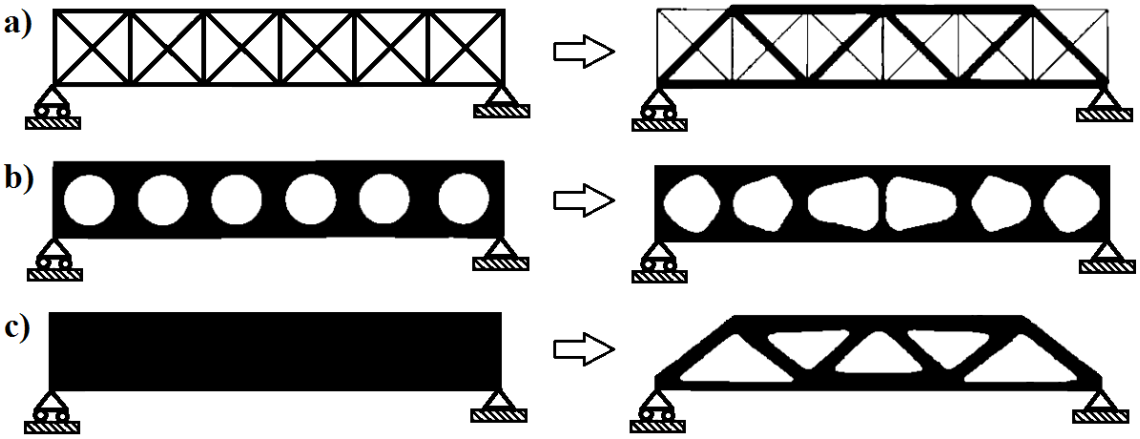

Figure 19. Material distribution based structural optimization methods. a) Sizing optimization of truss structure. b) Shape optimization c) Topology optimization

The beginning of modern structural optimization dates back to 1960 when Schmit established his paper about Structural Design by Systematic Synthesis at Conference on electronic computation. It was his work on use of mathematical programming techniques to solve nonlinear, inequality constrained problems that formed a base for development of modern optimization techniques. (Vanderplaats 1987) (Schmit 1960)

In 1988 Bendsøe and Kikuchi published their work on shape optimization technique later named Solid Isotropic Material with Penalization method (SIMP). Paper published by

Bendsøe and Kikuchi is considered as origin of topology optimization. (Bendsøe & Kikuchi 1988) The method originally proposed by them was developed to achieve designs with integer material distribution values of 1 (solid material) and 0 (hole).

Topology optimization is normally used to obtain preliminary design in early stage of product development. Typically in topology optimization objective function is compliance or mass which is minimized. The constraint functions are often local or global stress, mass fraction or deformation. Some very recent works have combined fatigue analysis into TO as constraint function. (Lee et al. 2015) (Oest & Lund 2017) (Jeong et al. 2015)

In this paper topology optimization is used to create improved boom head design subject to fatigue. This is done by reducing stress gradients at weld joint by obtaining a structure that distributes the stresses evenly to weld joint, avoiding high stress concentrations. The ultimate goal is to find engineering approach for utilizing optimization techniques in design of cast steel parts against fatigue.

5.1 Optimization theory

In this section, general example of topology optimization procedure is presented as proposed by Bendsøe in 1989. Topology optimization flow chart is shown below (Figure 20). The fundamentals of TO will be explained in more detail in following sections.

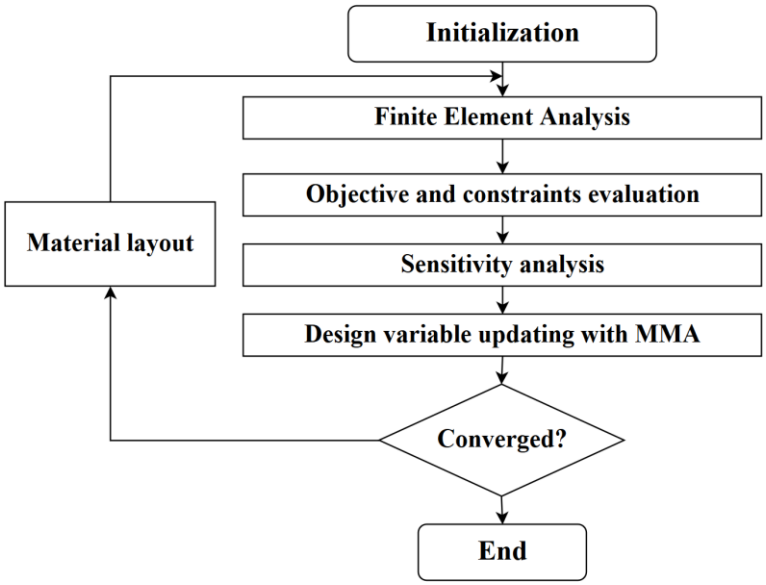

Figure 20. General topology optimization flowchart.

For topology optimization, the structure has to be discretized using finite element method. The discretized body will be subjected to application specific loads and other boundary conditions. During each optimization loop the objective and constraint functions are evaluated.

Design variable i.e. element density distribution is updated using optimization algorithm like method of moving asymptotes (MMA) to find the optimal material distribution. Resulted material distribution is checked against convergence limits and depending on result the loop will be restarted with redistributed material layout or optimization finished.

5.1.1 Problem formulation

Typical topology optimization problem in standard form can be written

$$\begin{aligned} &\min_{\rho} \boldsymbol{f}^T \boldsymbol{u} \\ &\text{s.t.}: \mathbf{K}(\rho)\mathrm{u} = \mathrm{f} \\ &\int_{\Omega_s} dV \leq V_s \end{aligned} \tag{18}$$

in which compliance ($\boldsymbol{f}^T \boldsymbol{u}$) is minimized subject to certain limited design volume percentage. Other than design volume constraints can also be used like stress and deformation constraints.

Bendsøe presents the structural topology optimization problem in its general form as problem of choosing optimal elasticity tensor $E_{ijkl}(x)$ that is variable over the design space Ω. In equation below

$$E_{ijkl}(x) = X(x)\bar{E}_{ijkl}, \tag{19}$$

$\bar{E}_{ijkl}$ presents the rigidity tensor and $X(x)$ is indicator that contains data of which elements have material or don't have material.

5.1.2 Penalization functions

Most common method for addressing variable element stiffness is variable density method SIMP presented by Bendsøe et al. Motivation for introducing SIMP method lies in problem of solving discrete valued optimization task where material is treated as 1 or 0, solid or void respectively. Solving this type of problem would require discrete optimization algorithm which would result in instabilities during the solving and ultimately can't be solved. (Sigmund & Petersson 1998) (Bendsøe 1989)

In SIMP method all the elements in the discretized solid model are assigned with variable density x_e. Relation between the density variable and Young's modulus (E) is then described with formulation

$$E_{ijkl}(x) = [x_e(x)]^p \bar{E}_{ijkl}, \tag{20}$$

where p is penalization factor. SIMP power-law needs to be modified to avoid stiffness matrix singularity that results when Young's modulus is zero. This has been implemented in:

$$E_{ijkl}(x) = E_{min} + [x_e(x)]^p (E_0 - E_{min}), \tag{21}$$

in which E_0 is the Young's modulus of the material and E_{min} is the minimum value of Young's modulus. Typically value in the scale of $E_0 * 10^{-6}$ has been used for minimum Young's modulus in literature (Oest & Lund 2017) .

Power law describing the relationship between density and Young's modulus and penalizes the material with lower densities making it more costly in terms of density/stiffness. The relation is illustrated in Figure 21. Power law makes optimization algorithm to favor the elements with density of one over those with lower density.

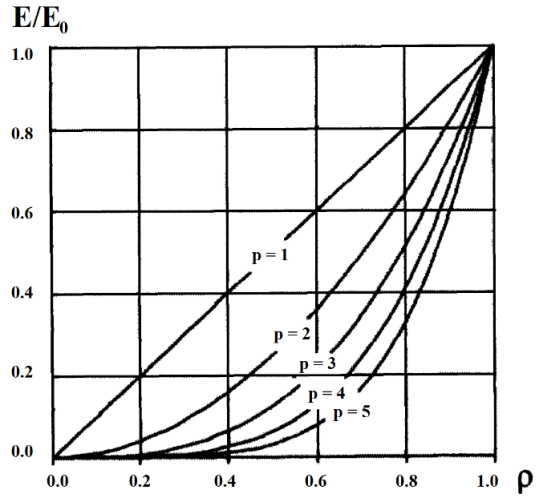

Figure 21. Specific material stiffness as a function of density with different penalization factors.

This method typically result into structure where material is 1 or 0, almost everywhere in the structure. Some problems that are encountered with this method are described in section 5.1.3.

Other material interpolation schemes have been introduced like Bi-directional Evolutional Structure Optimization (BESO) but in this paper we will not go into the details of other methods.

5.1.3 Design variable filtering

In density modification methods with hexahedron mesh checkerboard pattern can occur (Figure 22). Checkerboarding has been identified as finite element method based numerical problem. Optimization favors checkerboard structures due to its artificial stiffness. Filtering methods have proven to effectively remove checkerboard pattern from topology results.

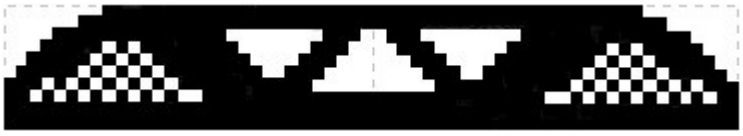

Figure 22. Checkerboarding effect on simply supported beam with center force.

Typical filtering method is weighted average method that has proved to remove checkerboard patterns from topology results. Method alters the design variable (x_e) of the element by taking weighted average of the neighboring elements from area of user specified radius *r* (22).

$$x_e = \frac{\sum_{j \in \mathbb{N}_e} \omega(\boldsymbol{x}_j) x_j}{\sum_{j \in \mathbb{N}_e} \boldsymbol{x}_j} \quad \text{where in} \quad \omega(\boldsymbol{x}_j) = 1 - \frac{\|\boldsymbol{x}_j - \boldsymbol{x}_e\|}{r} \tag{22}$$

This filtering based method was suggested by Sigmund (1994) and has been utilized effectively in topology optimization.

Checkerboarding can also be prevented by using higher order elements or tetra elements. However use of higher order elements results in substantial increase of computing time and is thus not favorable (see section 5.2). Other methods listed by Sigmund and Peterson are patches and smoothing. (Sigmund & Petersson 1998)

5.1.4 Stress constraint

Using stress constraint in TO is very costly. When stress constraint is used there will be immense amount of constraints introduced. Each node of each element would be constrained with stress limit, resulting in huge amount of constraints. Because of this problem, approximation methods for making the calculation less costly have been developed.

Three different stress constraint approximation approaches are typically used: local, global and clustered. In local approach the stress constraint is applied into every stress evaluation point (node) of the model resulting into excessive number of constraints.

Global method is at the very other end of stress constraint as in this method only one constraint is applied globally to the entire model. Neither of these two methods are practical as local method is computationally extremely consuming and global method is too inaccurate. (Duysinx & Sigmund 1998)

To address the problem of stress constraint, cluster methods have been developed. These methods are based on concept where the number of constraints are significantly reduced by combining stress evaluation points into clusters. Holmberg et al. in their paper explain usage of different clustering methods with case study. (Holmberg et al. 2013)

Typically the clustering is based on method where stresses from multiple nodes within specified radius around the center node are averaged to form one constraint for all the nodes within the range of the radius. Nodes that are within the radius form a cluster. This process is repeated for the entire model resulting into fever stress constraints and faster calculation. The clustering however has effect on accuracy of the result. Clustering can result in structure with local stress concentration peaks, as during optimization the clustering smooths these out by averaging the stress of several elements. For better accuracy the radius can be reduced, although with cost of computation time.

5.1.5 Optimization algorithms

In TO various different algorithms are used to solve the material distribution. The topology optimization problems are usually discretized with numerical method such as finite element method. This means that the explicit expressions of solutions are not usually available. Also the constraint functions and the objectives are usually non-convex and non-separable and thus direct optimization is not efficient method.

Due to aforementioned reasons the dual sequential approximation (DSA) methods are used for topology optimization. The workflow of DSA methods is shown in the Figure 23.

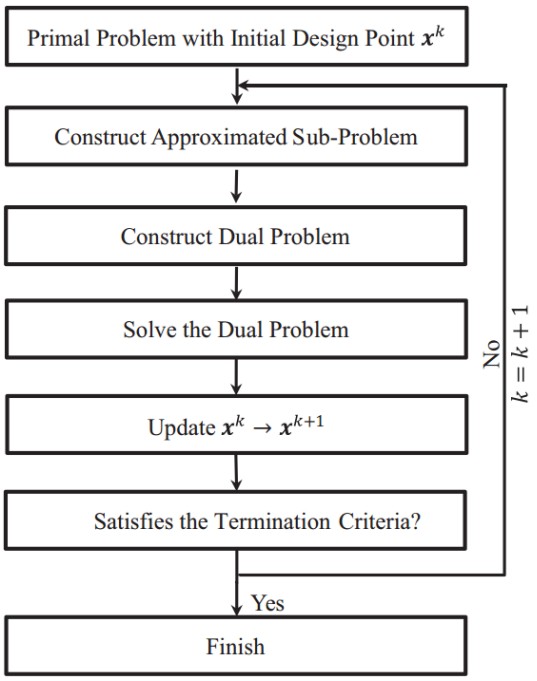

Figure 23. Workflow of DSA algorithm. Source (Li & Khandelwal 2014)

The DSA methods are based on constructing of convex and separable approximations of the objective and constraint functions in the current design point. The approximations form the sub-problem of the original problem. Sub-problem is then used to construct a Lagrangian dual problem which is then solved and checked against termination criteria.

For the formation of the approximation functions several different methods exist. These methods can be separated into three categories: local, mid-range and global approximation. In local approximations the function is built using only the information of the current design point which can be convenient sometimes. Li and Khandelwal list first-order, reciprocal, exponential and second-order approximations into the local approximation methods.

Mid-range approximations use not only the information from current but also from the previous iteration. This results into better approximation with little added computational effort. In mid-range methods a two-point exponential approximation is used.

In global methods method of moving asymptotes (MMA) is used. This method was originally proposed by Svanberg. He extended CONLIN method to form MMA. These methods are explained more accurately by Li and Khandelwal and the original authors.

MMA is likely the most used algorithm in TO, but recent studies have shown better computational performance with extended MMA based optimization algorithms. Li and Khandelwal proposed extended MMA algorithm to improve its computational performance. The performance of different algorithms was also compared with some test structures. (Li & Khandelwal 2014) Some papers suggest also use of genetic algorithms for optimization algorithm in TO.

5.2 Other important aspects

In topology optimization use of higher order elements is generally not necessary. Higher order elements have mid-side nodes which allow the sides of elements to be curved to fit better in the geometry. (Figure 24)

Higher order elements result into more accurate analysis results in FE analysis but in TO it is not considered necessary. Instead it is recommended to use first order elements with finer mesh. In TO the level of details attained in the result is limited by the size of mesh. Higher amount of elements gives higher level of design freedom. The higher order elements affect the computing time by making it more time consuming. This effect was demonstrated with simple structure.

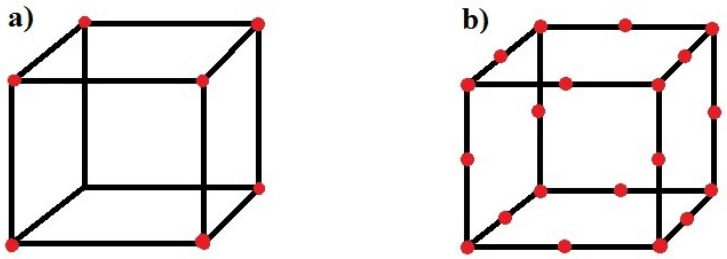

Figure 24. a) 8 node linear hexahedron element. b) 20 node quadratic hexahedron element

The effect of element type on performance of GENESIS optimization software was tested with simple L-shaped bar. The bar had all degrees of freedom (DOF) fixed on the top and vertical force on the tip of the bar.

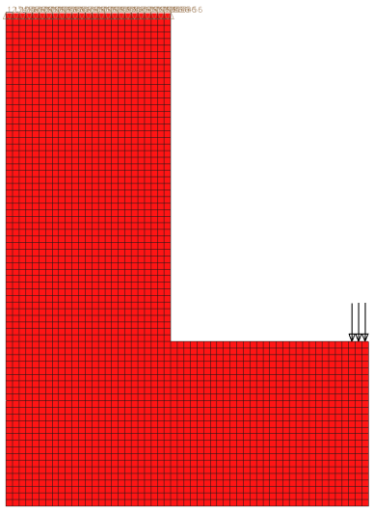

Figure 25. L-bar structure used for testing the software.

The effect of element type on computation time was studied with the structure shown in Figure 25. Bar was meshed with linear and quadratic hex elements and optimized separately. Computation times were recorded and results are shown in Figure 26.

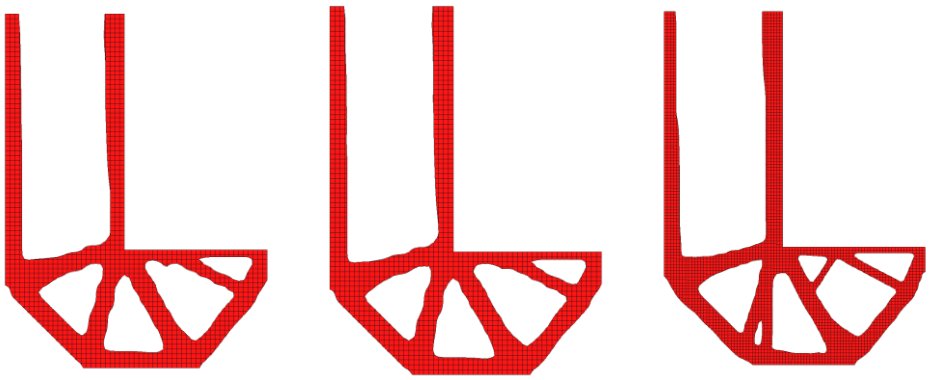

Element type	Quadratic	Linear	Linear
Element size	1 mm	1 mm	0.65 mm
Element number	26250	26250	101712
Nodes	30316	30316	111520
Computation time	16 min 29 s	2 min 41 s	15 min 37 s

Figure 26. Computation times on simple L-bracket with quadratic and linear elements and different mesh sizes.

It is shown that with same structure discretized with equal linear and quadratic mesh result in significant difference in computation time. The material distribution results however are identical, regardless of the element type. It was also tested how much finer mesh would result the same computation time as the 1 mm quadratic mesh. When using finer mesh more refined structure can be achieved, as seen in the figure above.

Computation time was reduced to one eight of the initial computation time when elements were changed from quadratic to linear. If finer details are not desired, the size of members can be limited to achieve less complex structures.

5.3 Fatigue constrained topology optimization

Some recent works have been published on fatigue constrained topology optimization. In procedure presented by Oest and Lund the time-varying stresses are found with means of linear superposition. Reference load is applied to structure and stress states at other time steps are defined by linear interpolation. Fatigue constraint is subjected to each element or element cluster in similar manner as in stress constraint. The fatigue life of each element is optimized against user defined level of damage sum.

Oest and Lund demonstrated fatigue constrained TO using Sines method for combining multiaxial stresses and Palmgren-Miner rule as fatigue accumulation formulation. To achieve 0 – 1 topology density plot, they also applied P-norm (power rule) method to Sines fatigue damage rule. (Oest & Lund 2017)

Another approach is to define maximum acceptable stress range peak for desired fatigue life of the structure. For constant amplitude stresses this can be done using simply S-N curve. For variable amplitude stresses more complicated approach is needed. The known stress spectrum has to be used to calculate the damage sum for the spectrum. This damage sum is then compared to maximum allowable damage sum to determine highest allowable peak stress range in the spectrum. Regardless of load type the maximum stress range peak is paired in analysis with the corresponding load condition. Other constraints for the TO problem is then formulated and the problem can be solved. This method for variable amplitude load was used by Holmberg et al. in their paper and demonstrated with simply supported beam. (Holmberg et al. 2014)

5.4 Topology optimization with GENESIS

GENESIS topology optimization is commercially available software developed by Vanderplaats Research & Development Inc. (VRAND). The software includes topology, topography, freeform, sizing and topometry optimization tools and is available as ANSYS extension.

Genesis GUI in ANSYS workbench allows user to set up optimization problems using typical ANSYS setups. The software supports nonlinear analysis settings including joints. However some restrictions are set by the software. When using symmetry constraint with non-symmetric mesh, genesis TO solver requires specifying of minimum member size. Genesis recommendation for minimum member size is at least 2-3 times the size of the elements used in the model.

The performance of the software is shown here with some examples. Effects of different penalization function values and stress constraints on simple structure is demonstrated using Genesis. The GUI is not explained here. VRAND doesn't offer any further information of the algorithms they use in their software and therefore it won't be discussed here either.

5.4.1 Power rule

Genesis uses density based method in topology optimization. Genesis allows user to choose the penalization factor, but recommends a value between 2 – 3. The effects of different penalization factor values were tested on simple L-shaped solid geometry. This type of structure is commonly used in testing TO algorithm performance and functionality. In section 5.1.2 the basic theory of penalization function is explained and the effect on stiffness is visualized with graph. Different penalization values were tested using Genesis. The problem boundary conditions are shown in Figure 25. The beam was subjected to a force on the tip of the L. The top surface of the L had all DOF fixed.

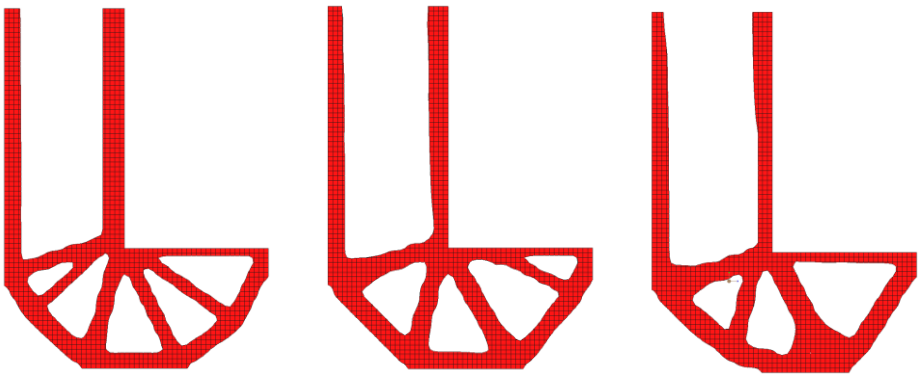

P	2	3	4
Iteration count	18	14	12
Computation time	6 min 6 s	2 min 41 s	4 min 49 s

Figure 27. Effect of penalization function value on computation time and structure.

The results obtained with different penalization factors are shown in Figure 27. Penalization function value of 1 was also tested. That resulted into un-acceptable design and is therefore not presented here.

It can be seen that with smaller p-value the resulting structure has higher genus. Smaller p-value also took longest to solve while p = 3 converged fastest. These results support the guidelines given by VRAND.

5.4.2 Stress constraint

GENESIS has various stress constraints available as built in feature including von Mises, major principle, normal and shear stresses. If the optimization is performed with no stress constraint and the stiffness is maximized, the structure will usually have high stress concentration peaks. The effect of various stress constraints is shown with the same example structure as previously.

The effects of different stress constraints were studied using fully reversed vertical force induced into the tip of the L-bar. Genesis allows user to set up custom constraints using synthetic response tools in Genesis design studio. In this example synthetic response was set up for maximum stress range. Major principle stresses in both time steps were recorded and the range was calculated.

Optimization results with different constraints are shown in Figure 28. To keep the structure 2D, manufacturing constraint was set up. The structure was meshed with linear tetra mesh and penalization factor was set to default value (3).

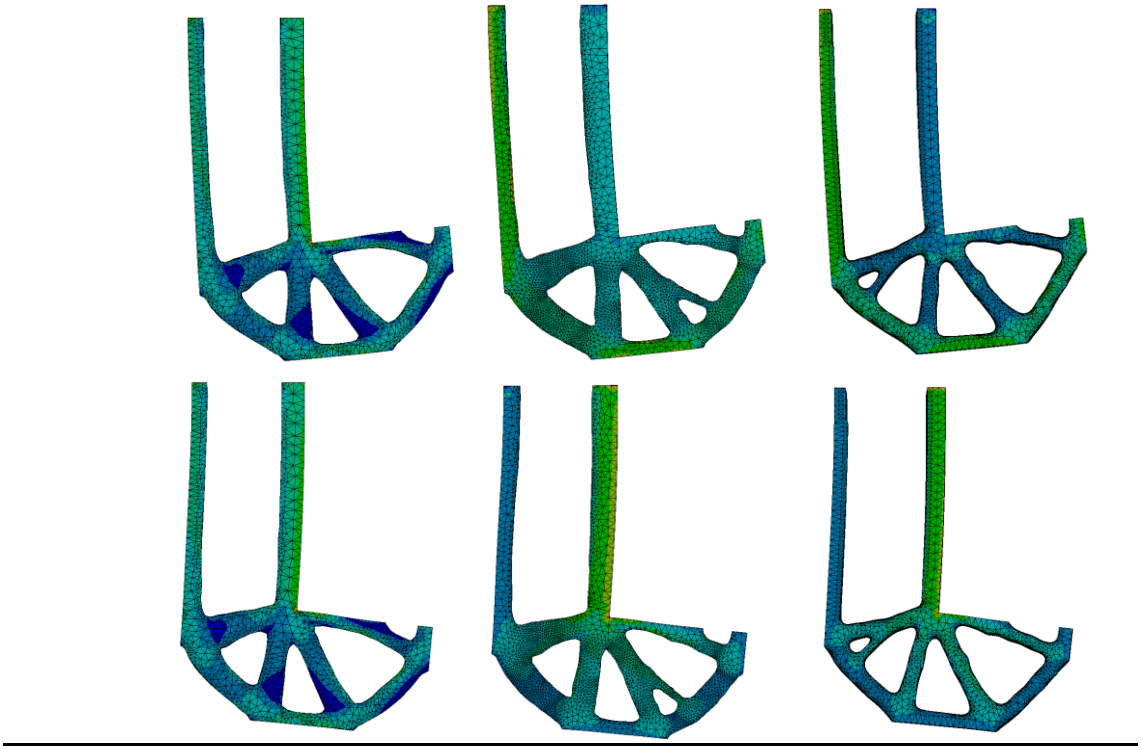

Stress constraint	Von Mises	Maximum principal	Stress range
Stress limit	150 MPa	150 MPa	UB 130 MPa, LB -130 MPa

Figure 28. Stress constrained TO-results with L-beam. Figures shown in deformed form with stress color graphs.

Resulting structures are significantly different depending on the constraint. When compared to same structure with no stress constraint (Figure 27) the difference is even greater. Stress constraint reduces stress peak at the tip of the structure where the force is applied. Due to stress clustering, the high local peak stress in the inner corner of L-plate is still present after optimization. GENESIS does not allow modifying the clustering radius.

It is worth mentioning that without stress constraint the optimization of the L-bar took only 2 minutes 41 seconds as with von Mises constraint computation time was 42 minutes 52 second. This demonstrates the computational expense of stress constraint.

6. CASE STUDY

The goal of this thesis is to develop a simple and easy to use method for designing cast steel structures such as the boom head so that they fulfill the fatigue life requirements.

Figure 29. Original C44+ boom head design with V-shaped weld joint interface.

In this paper we are utilizing ANSYS 18.1 with GENESIS topology optimization in order to minimize the stress at weld by optimizing the shape of the boom head and the weld joint location. Constraints, other than the stress, are mass which must not exceed that of the previous design. The work flow of the optimization process is shown in Figure 30

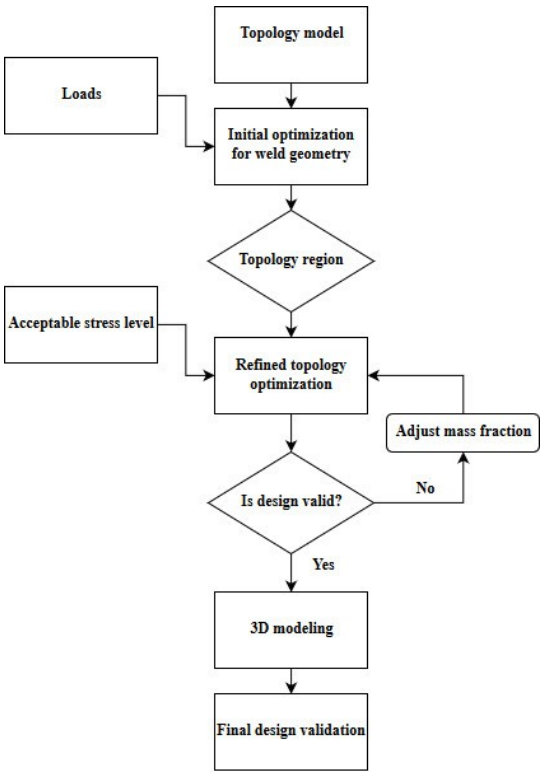

Figure 30. Suggested flow chart of designing cast steel parts against weld joint fatigue.

The preliminary design was first derived with ANSYS Screening method where set of acceptable weld head seam angle and head length combinations was made. Each combination was optimized with topology optimization and the resulted stresses at weld were observed.

In refined topology optimization the best preliminary design was further optimized against fatigue damage function subjected to weld joint in order to achieve structure with required fatigue life. The topology result was then validated by first creating smoothed solid geometry using SpaceClaim design modeler. Smoothed model was used as template for modelling the boom head using SolidWorks.

The new optimized boom head design was put into crane assembly FEM model and analyzed against worst case loads. Sub-model of weld joint with ENS weld geometry was modeled and analyzed. Finally stresses at weld root of the optimized structure were compared to those of the original structure.

7. HARVESTER

Ponsse Oyj was founded in year 1970 when Einari Vidgrén built his first forwarder type forest machine in Vieremä Finland. Ponsse is one of the leading cut to length forest machine manufacturers in world. The company product portfolio consists of harvesters, forwarders and processing heads.

During the first years of operating the company focused on forwarders that were used to collect logs from forest and transported to road sides until the year 1985 when first harvester head H520 was developed. Modern harvester (Figure 31) is machine that does felling, delimbing and cuts the tree to desired length logs. Tree processing is done by harvester head mounted into crane.

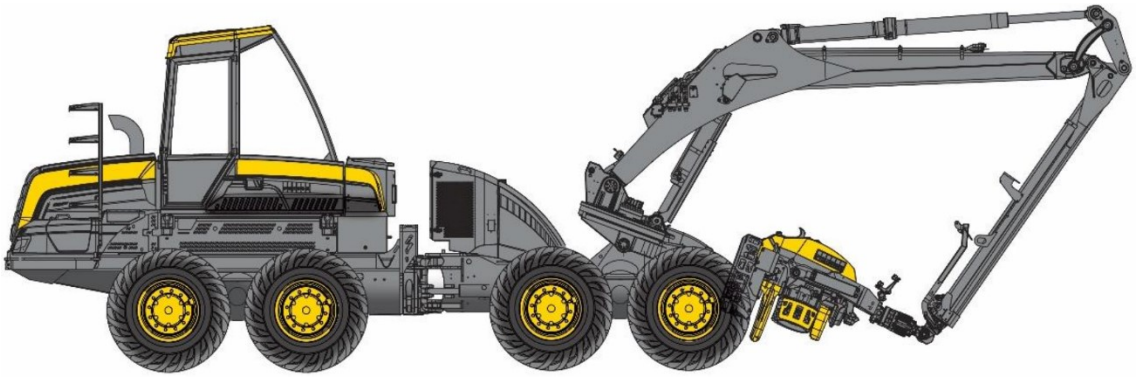

Figure 31. Eight wheeled Ponsse Beaver harvester machine with C44+ crane.

7.1 Harvester crane

Ponsse harvester cranes are separated into two types, sliding boom cranes and parallel cranes. Harvester cranes are hydraulically powered and divided into different types and models by their controlling principles and load handling capacity.

In this case study we focus on lifting boom cast head of parallel crane C44+. The crane has maximum slewing torque of 57 kNm and maximum lifting moment of 250 kNm. Maximum reach of the crane is 11 m.

7.1.1 Operational cycle

Typical cut to length (CTL) harvester machine operating cycle consists of tree felling, delimbing (or snedding) and bucking.

During the felling operation the harvester head grapples around the tree stem close to ground. The saw blade then cuts the tree while crane lifts the tree to prevent blade jamming between stump and trunk. Forest machine operator also simultaneously pushes the tree to control the direction into which the tree falls. Tree is allowed to fall freely on ground while the machine holds it from its stem.

Felling is followed by delimbing process. The purpose of delimbing is to effectively remove the branches from tree. Harvester head feed rollers pull the tree through the harvester head. Debranching blades are pressed against the tree and while pulled through the head the blades cut of the branches.

Figure 32. Harvester head. Yellow debranching blades and spiked feed rollers are visible.

During the delimbing process the tree is also cut into specified length. This step is called bucking. When the tree is cut to length the cut end falls freely on to the ground.

C44+ crane is used in many different countries and also for eucalyptus tree harvesting. Processing eucalyptus tree differs from that of pine or spruce. Eucalyptus tree has significantly less branches than for example spruce and the branches are only at the very top of

the tree. Special characteristic for eucalyptus harvesting is the need for removing the bark of the tree directly after felling.

Debarking the eucalyptus tree is done using harvester. The process requires running the tree back and forth through the harvester head in order to remove the bark. Due to this operation the booms in eucalyptus harvesting are subject to higher amount of loading cycles per tree than boom used for spruce and pine harvesting.

According to field tests the highest stresses are induced during tree felling process when the operator uses the crane to direct the tree to desired direction. During felling the harvester boom slewing torque and lifting pressure limits are typically reached. High stresses are also present when big trees hit the ground.

7.2 Boom head design

Traditional boom head constructions are welded plate structures, where the head consists of several laser or plasma cut steel plates that have been bent and then welded to form a boom head. Boom head parts are welded on the boom main structure. After welding process the whole boom structure is machined to required tolerances to fit bearings and other components requiring high accuracy.

Ponsse C44+ boom has been designed with single piece cast steel boom ends, including the boom head. Cast head and the boom main structure is joined by butt weld. After the parts have been joined the whole boom undergoes machining process, just like plate structure, for accurate locating tolerances of components.

Plate boom heads are used by several forest machine manufacturers. Similar plate designs are also typically used in excavator cranes. This type of boom head has typically side plates that are welded on the main boom, center piece in the front to increase torsional stiffness and through-hole tubing or turned sleeves to accommodate the sliding bearings.

Cast boom head design consist of single piece structure that is joined in to the main part of the boom by butt joint. Cast boom head allows very complex shapes to be used. Casting allows variation of thickness in all directions through the head. This way stresses in the structure can be distributed effectively around the head. In cast structure there is also less weld joints which are prone to fatigue failure. Lesser weld joints also make manufacturing easier and faster.

8. OPERATING CONDITIONS

Ponsse harvester are sold worldwide to very different operating conditions. Some machines are operated on eucalyptus tree fields in Brazil when other machine spends lifetime in forests of Siberia. This sets us into difficult position where we need to design structure against worst case loading.

In this work we focus on operating conditions that were measured in Canada. Measurements were made in 2016 with Ponsse Ergo, 2015 series, equipped with C44+ crane and H7 harvester head.

8.1 Measured load data

The load condition of the boom has been tested by strain gauge measurements at field operation conditions. Strain measurements have been made in various operation environments including typical Finnish and Canadian forests. Somewhat big differences in the induced stresses has been reported between different operators and operating environments.

The length of the measured operating cycle was just under 6 h including all typical operations that occur during normal use of the harvester. The measured data was modified to be nCode compatible and the strains were transformed into stresses. Data was processed using nCode and Excel.

8.1.1 Acceptable stress level

Minimum life time requirement for the forest machine is 20 000 h. Field measurements include all the phases of the process, including low stress states like moving from tree to tree. The strains on the boom have been measured on the spar of the boom at the vicinity of boom head. (Figure 33)

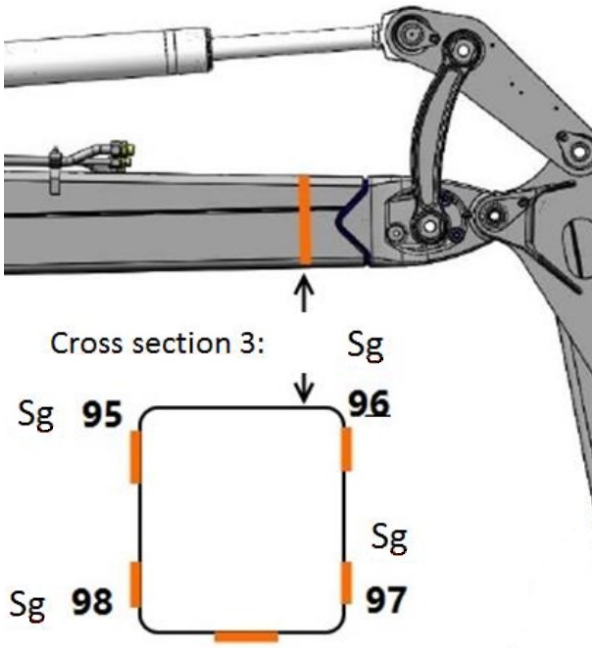

Figure 33. Location of strain gauges at C44+ boom spar.

Strain gauges were located close to the weld root and thus the measured strain spectra distribution is assumed to represent the strain distribution at weld toe.

Rainflow strain cycle counting was performed for each gauge using nCode Glyphworks. Omission of non-damaging assumed stresses was performed, stresses below 10 MPa at each strain gauge were discarded. Minimum amount of cycles in 20 000 h service life T_{sl} was then obtained by dividing service life with un-omissioned length of the stress sequence $L_{spectra}$, formula (23)

$$N_{service} = \frac{T_{sl}}{L_{spectra}} \tag{23}$$

Typically Palmgren-Miner rule is used for determining how many cycles the structure can hold with given stress. In this work we need to find level of stress spectra that gives us life of $N_{service} = 3466$ cycles. By scaling the rainflow stress sequence data with factor n we can find the stress level that fulfills our service life requirement.

First maximum value for damage sum of one cycle was obtained by dividing specified maximum cumulative damage sum $D_{limit} = 0.5$ by $N_{service}$. D_{limit} value was chosen according to IIW recommendations for welded structure subject to VA loading.

$$D_{spec.max} = \frac{D_{limit}}{N_{service}} \tag{24}$$

To evaluate the actual acceptable stress level we introduced correction factor n. This factor is used to scale the Rainflow stress ranges so that damage sum is equal to $D_{spec.max}$. Scaling was done using Excel solver function.

The case representative SN-curve was approximated by two separate power functions, before and after knee point (Figure 34) to automate damage sum calculation in Excel.

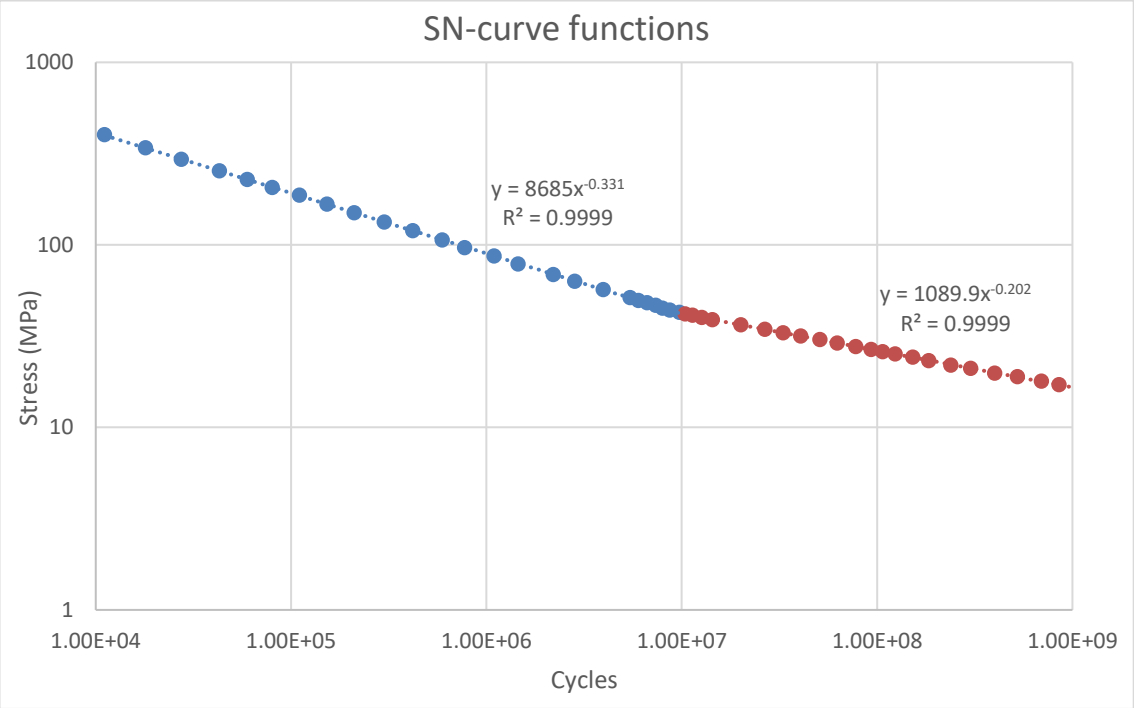

Figure 34. IIW recommendation for SN-curve with variable amplitude multiaxial load spectra (FAT 71).

Damage sums for stresses below and above the knee point were calculated using formulas below.

$$D_i = \frac{n_i}{1.08785 * \frac{10^{15}}{n * N_i^{\left(\frac{500}{101}\right)}}}$$

$$D_j = \frac{n_j}{7.93609 * \frac{10^{11}}{n * N_j^{\left(\frac{1000}{331}\right)}}} \tag{25}$$

$$D_{spec} = \sum D_i + \sum D_j = D_{spec.max}$$

Where subscript i and j are stresses below and above knee point respectively. Above equations were solved with Excel solver and scaling factor n was obtained. Scaled stress spectrum was formed and maximum stress range value σ_{max} was calculated (Table 3).

Table 3. Values for determining the acceptable maximum stress level.

Acceptable stress level						
Service life **[h]**	L_spectra **[h]**	N_spectra	D_max	D_spec.max	*n*	σ_max **[Mpa]**
20 000	5.77	3466.205	0.5	0.000144	0.93028	131.3

From scaled rainflow chart we can take the maximum stress range and use it as stress constraint in topology optimization of the boom head. In rainflow cycle count the maximum stress is the maximum stress range. In rainflow the local tensile and compressive stress together form the range, therefore fully reversed maximum load condition has to be analyzed with FEA and stress range formed from maximum and minimum stresses per element.

To formulate the range and exponential relation of stress and fatigue life into optimization a function of damage sum and stress scaling was made. Damage sum for the spectrum was calculated with different stress scaling factors and resulting damage sums were plotted. Power function was fitted into those values to form function of damage sum and stress scaling factor.

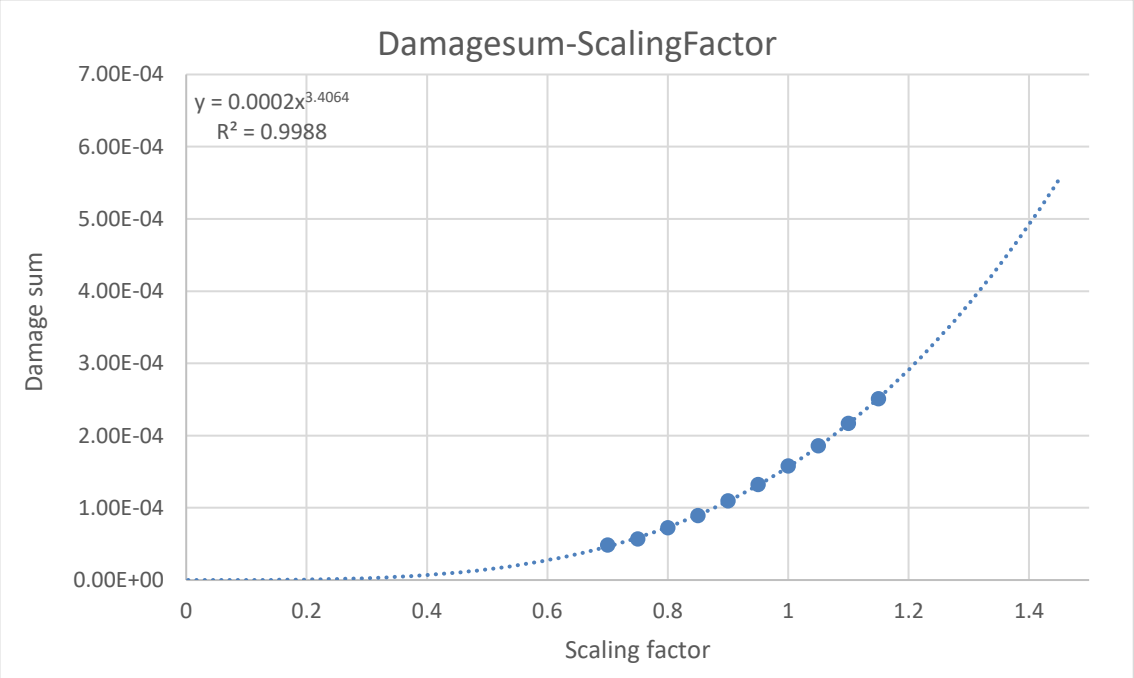

Figure 35. Figure of damage sum as a function of stress scaling factor.

The fitted function (26) describes the relation between stress and fatigue damage. The function is later used to formulate the constraint used in optimization.

$$D_{spec} = 0.0002 * n^{3.4064} \quad (26)$$

In optimization the scaling factor n is derived by evaluating normalized stress range at weld seam. Range is calculated per element from normal stresses acting perpendicular to weld seam with two load cases representing fully reversed load. The stress range is then divided my maximum peak stress range of the original measured stress range spectra. (See section 9.2.1)

In weld fatigue the initial weld condition, weld type and material have significant effect on fatigue life of the structure. These effects have been considered by choosing the D_{limit} value according to current recommendations by IIW. For more accurate result, fatigue damage model should be calibrated by fatigue testing using the actual load spectrum and the actual structure. Making this type of testing is very time consuming and expensive. In this thesis calibration was not performed. Even without the calibration it is possible to define whether the structure has been improved in terms of fatigue.

Sample of the original stress-time data and the rainflow stress spectra is given in appendices.

8.1.2 Load conditions

The load state at the boom is determined using the original boom design. Original boom design has been modeled and simulated with ANSYS 18.1.

By previous experience and field measurements the most critical load conditions has been found to be operating conditions where boom is at 90 degree angle (Figure 36) and where the boom is at its maximum reach (Figure 37). Both of these operating conditions have been modeled in ANSYS workbench separately. According to measured strain data the maximum stresses are observed during tree felling. During tree felling, the harvester head holds the tree from the stem. Tree is lifted to avoid blade jamming and pushed to guide it to desired felling direction.

Field measurements have shown that in typical operating conditions lifting force and rotating force exceed their maximum value. Joint forces have been derived from analysis model where the rated maximum lifting force and maximum rotating torque have been

scaled by factor proven with previous experience. Torque of 65 kNm and lifting force of 462 kN were used.

In both simulations the boom head (point A in Figure 36) has translations fixed in global Y and Z directions. Two joint forces, lifting force and moment, are then induced at the base of the crane. The boundary conditions for both operating conditions are illustrated in Figure 36 and Figure 37.

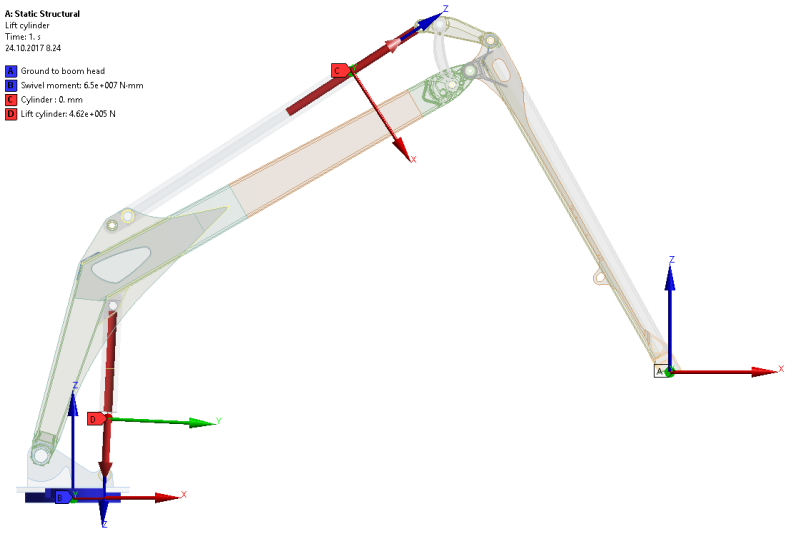

Figure 36. FEM model of C44+ boom at 90 degree angle. Boom head (A) is fixed and forces are applied through joints B and D.

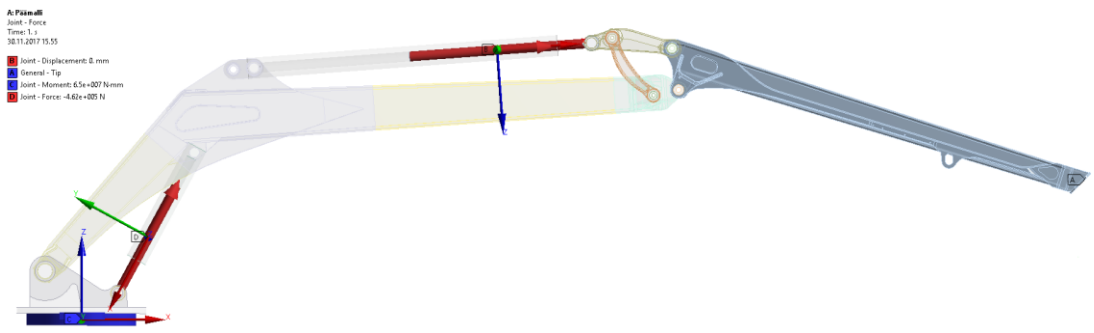

Figure 37. FEM model of C44+ boom at maximum reach. Boom head (A) is fixed. Loads are applied through joints C and D.

After running the simulation with the forces stated above the reaction forces at boom head were reclaimed from both models (Figure 38 and Figure 39). The reaction forces are used in optimization so we can run the optimization for smaller sub-section of interest. Direction of each reaction force can be visualized from the figures.

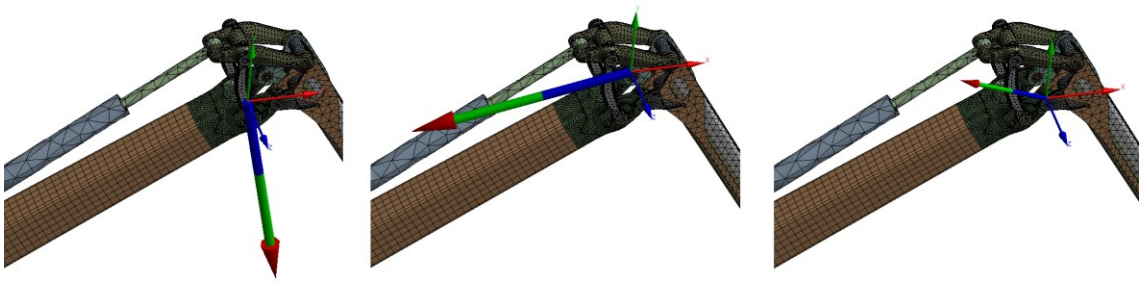

Figure 38. Reaction forces at lift boom joints with boom in 90 degree angle.

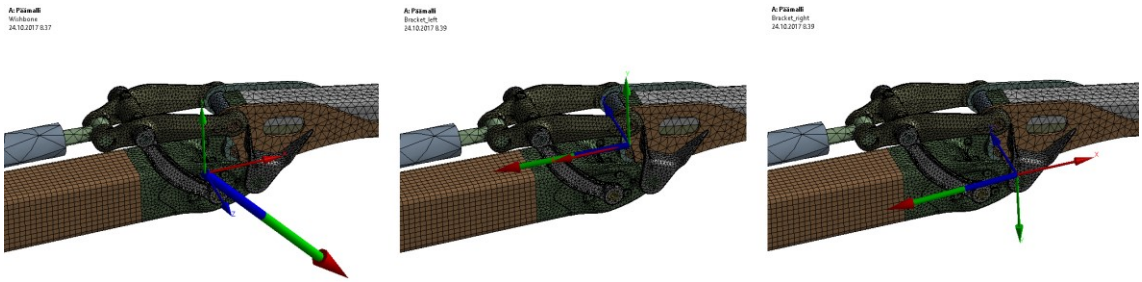

Figure 39. Reaction forces at lift boom joints with straight boom at maximum reach.

Boom head joint surfaces, on which the loads are acting, are named *Wishbone*, *Bracket_left* and *Bracket_right*. Loads for each surface are listed in table below. It is important to notice that forces are transformed into global coordinate system.

Table 4. Reaction forces at boom head in both load conditions. Loads are given in global coordinate system.

Load condition	Loaded surface	X [N]	Y [N]	Z [N]
Boom 90 degree	Wishbone	47851	-235210	-1278
	Bracket left	-60218	-18439	-7628
	Bracket right	-176220	84128	19387
Boom straight	Wishbone	12500	-14864	-2008
	Bracket left	-76270	-4229	-9436
	Bracket right	-236350	1842	12950

9. DESIGN OPTIMIZATION

Original C44+ boom head design has V-shaped weld joint (Figure 29). This shape has some drawbacks in manufacturability and would be beneficial if it could be replaced with straight joining surface.

First step in optimization of the boom head was to define the optimal joint geometry. This was achieved by screening optimization method where different joint angles and lengths were analyzed with topology optimization and stress minimization objective. After screening for different weld joint geometries, the new shape was used in final topology optimization against fatigue.

9.1 Geometry optimization

To define optimal shape for weld joint geometry the boom head 3D-model was parameterized. Two parameters were defined to modify the shape of the boom head. Special area of interest is the possible V-angle of the weld joint area. Second parameter was total length of the cast boom head. (Figure 40)

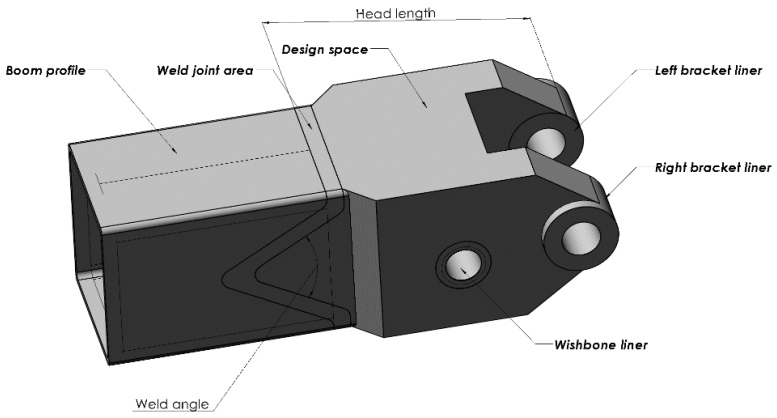

Figure 40. 3D model for preliminary geometry optimization.

Boom profile represents the shape of actual square beam that is used in boom. The length of boom profile has to be enough to allow the stresses caused by restricted warping to be leveled out.

Weld joint area is used as control area for stresses. Separate body is needed due to software restrictions. This area is not optimized by topology.

Design space is the maximum volume the part can occupy to be functional. The shape and size of the section is restricted by shape of boom profile and the head of second section of the crane.

Wishbone liner and *left* and *right bracket liners* were also separated from topology optimization. Sizes of the liners were defined from original boom head design.

Head angle and *head length* are the optimization design variables.

The goal was to minimize the maximum stress at weld joint area. Geometry of weld profile (See Figure 43) was not modeled into initial boom head weld geometry optimization as the stress concentration effects of ENS are not assumed to be dependent on the angle at which the load is applied to it.

All the different combinations of given angles and head lengths were simulated and results were recorded.

Table 5. Discrete geometry parameter values used in geometry optimization.

Angle	60	70	90	140	179
Length	350	400	450		

For topology optimization it is necessary to define maximum design space. The boom head for optimization was modeled using SolidWorks 3D modeler. Head was separated into six individual parts shown in Figure 40.

The geometry of boom head was optimized with combined topology optimization and geometry optimization. In the optimization routine the topology region geometry is changed after converged topology optimization. (Figure 41) For each topology optimized geometry the maximum and minimum stresses at weld joint area were recorded and the best design was chosen among the results.

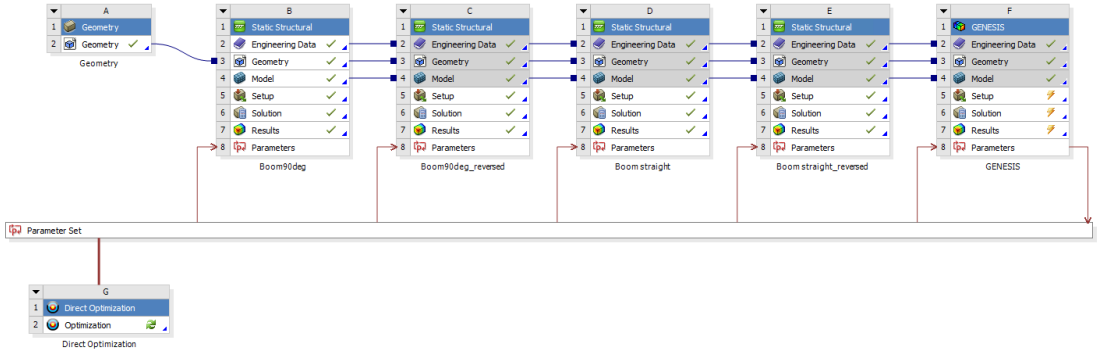

Figure 41. Initial optimization workbench schematic. Geometry values are set as inputs for each module and stresses as output from GENESIS.

9.2 Optimization against fatigue

Geometry optimization show that the best design for boom head weld is straight joint. To find optimal topological shape for the boom head, the design from initial geometry optimization was further optimized with GENESIS TO.

Geometry and meshing used in final TO is shown in Figure 42. The head is split into multiple sections of which red sections are optimized. Grey region is the weld joint area which has the fatigue constraint.

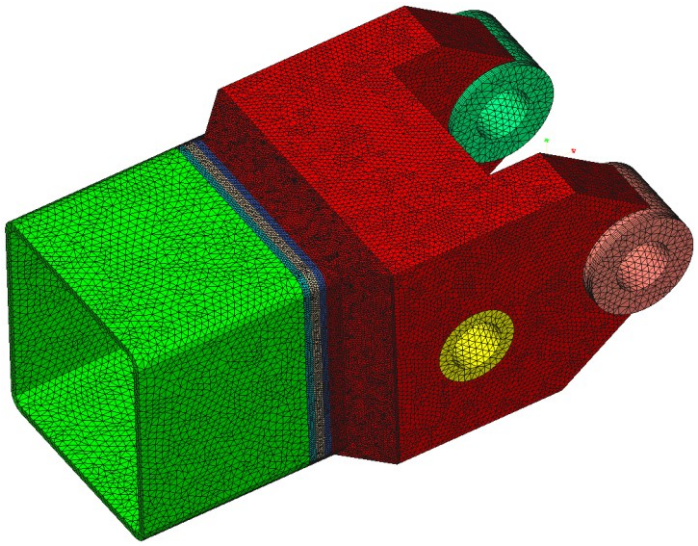

Figure 42. Topology region of boom head in GENESIS Design Studio.

9.2.1 Boundary conditions

Optimized region in TO is shown in the Figure 42 with red color. Boundary conditions and objective function was subjected into this red region. Topology mass fraction constraint was set to 0.3 and objective was set minimizing compliance (maximizing stiffness). Topology mass fraction was set to 0.3 which yields in approximately same final mass as the original boom head design. Other constraints were symmetry in YZ-plane. For convergence limit setup the default settings were used.

Novel approach for utilizing effective notch stress method for final stress constrained topology optimization was used. The weld geometry was modeled with 3D-modeler according to IIW recommendations for ENS method (Figure 43). The width of the root is

determined according to the actual weld. The root opening between head and spar is prior welding 3 mm resulting in width of approximately 4 mm at root reinforcement.

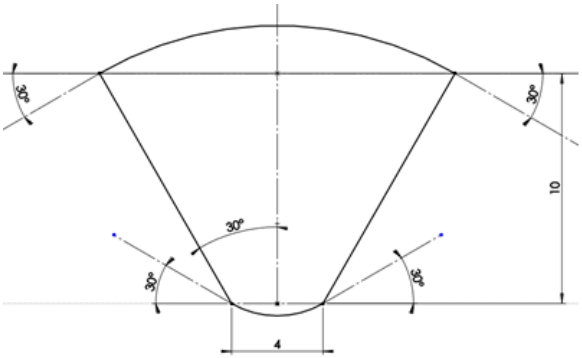

Figure 43. Cross section view of the modeled weld geometry according to IIW recommendations for ENS method.

Radius of 1 mm was modeled into the weld root according to recommendations by IIW for ENS method. (Hobbacher 2016)

Due to use of linear elements in TO, meshing the weld joint according to requirements of ENS would be computationally expensive. The geometry is assumed to behave linearly with the stresses subjected to the structure. Thereby the notch effect of butt weld was implemented into the formulation by defining a stress concentration factor with unit load.

The stress concentration effect of the weld geometry was studied in separate FEM analysis (Figure 44). This factor was then introduced directly into the stress range of the fatigue constrained TO analysis (27).

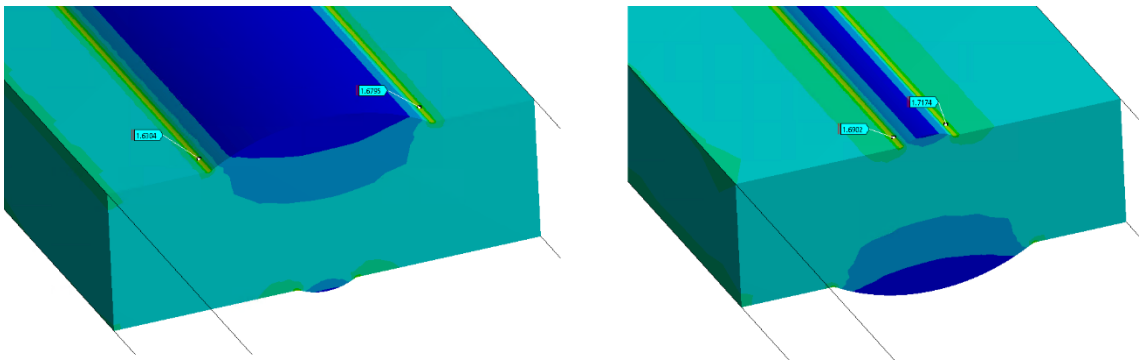

Figure 44. ENS modeled stress concentration factor on weld cap and weld root.

Fatigue constraint function for topology optimization was formulated as stated in following equation.

$$D_{spec\_max} = 0.0002 * ((ABS(\sigma_1 - \sigma_2) * 1.7)/141)^{3.4064}, \qquad (27)$$

Where D_{spec_max} is the maximum allowable damage sum of the spectrum, σ_1 and σ_2 are normal stresses acting perpendicular to the weld joint in fully reversed worst case load

cycle. Constant 1.7 is the stress concentration factor derived with ENS method. Divisor 141 (MPa) is the maximum stress in measured rainflow data.

Weld joint geometry was split into three parts with equal sized mesh. Fatigue constraint was introduced into the middle section at weld joint to ensure mesh compatibility and reduce the effect of stress clustering in TO. The topology region was also split into two parts where part next to weld joint was meshed with finer mesh to achieve finer details close to the weld joint area. Element size of 6 mm was used in coarse part and 3 mm in finer meshed section. This allows minimum member size of 12 and 6 mm respectively.

9.3 Structure verification

After topology optimization the model was exported into .STL file. The model was smoothed using ANSYS SpaceClaim and shrinkwrap tool. Different smoothing settings were tested to obtain desired shape and to close small gaps and smoothen sharp mesh edges.

Smoothed TO result was used as reference for modelling new boom head design. The design was modeled to match as closely to the optimized result as possible, without concerning the manufacturability of the design.

New boom head was paired with the original boom spar and complete model of the C44+ boom in straight and 90 degree position was simulated using ANSYS. Weld joint was modeled with ENS method and a sub-model was created. Sub-model was analyzed and the maximum stress ranges at weld root were recorded in both boom positions.

10. RESULTS

Optimization was run in GENESIS design studio. The optimization result is shown in Figure 45.

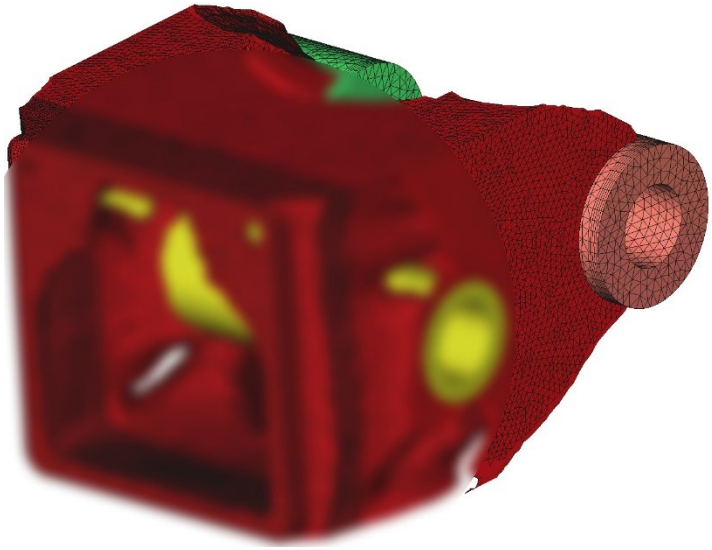

Figure 45. Optimized boom head geometry.

The computation time for final topology optimization was 16 hours with 12 iterations to convergence. Optimization result shown here has mass fraction of 0.3 of original mass. Weld joint and boom spar is not shown here for better visualization of optimized structure.

Topology optimization result was used as a template for modelling the new boom head for final stress analysis. The design used for final stress analysis is shown in Figure 46. The new head design has weight of approximately 100 kg, being 4 kg lighter than the original structure.

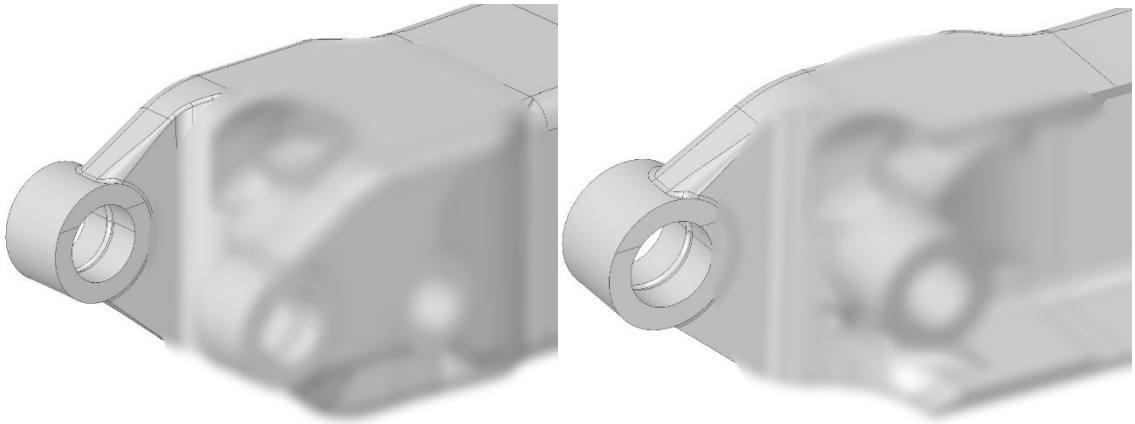

Figure 46. Optimized boom head design used for stress analysis.

10.1 Comparison

Stresses in the weld of the original boom head and new optimized design was compared by creating complete analysis model of the boom and using sub-model with ENS for weld joint. The results are shown in following figures.

In all cases the stresses are recorded on the root side of the weld. The fracture has been proven to start from root side of the weld.

Structure	Boom 90 deg	Boom straight
Stress range		
Backing	214.226 MPa	260.07 MPa
No backing	120.548 MPa	105.587 MPa

Figure 47. Simulated effective notch stresses at original boom head design with and without weld backing. Left column shows the stresses with boom in 90 degree angle and right column stresses with straight boom.

Stresses in original structure were observed with backing bar which is current design in production. Original design was also analyzed without backing bar for reference. The stresses are normal stresses perpendicular to weld joint.

Weld joint stresses with new design are shown in Figure 48. The stresses are normal stresses in x-direction (perpendicular to weld).

	Boom 90 deg	Boom straight
Stress range	33.66 MPa	118.437 MPa

Figure 48. Stresses in weld joint of optimized structure with boom in 90 degree angle and straight boom.

10.1.1 Observations

Results show clear reduction in stress level at weld joint, resulting in improved fatigue life of the structure. Current structure has stresses of 214 and 260 MPa with 90 degree and straight boom, when corresponding stresses with new structure are 34 and 118 MPa. When comparing optimized design and original design without backing the difference is not quite as significant. Original design without backing has stresses of 121 and 106 MPa.

It is shown that with optimized design the maximum stress range is degreased slightly compared to original structure without backing bar. With straight boom the stress range is increased slightly but the maximum tensile stress is reduced from 34 to 12 MPa. In terms of fatigue life the tensile stress perpendicular to weld joint is more harmful than compressive stresses. Stress perpendicular to weld joint is the driving stress for the crack opening, mode I crack which is the most harmful.

Fatigue failure on field has started with current design from the same location where maximum stress in FEA analysis is present (Figure 47). In 90 degree angle operating condition high normal stress range is subjected into the original structure at the area of maximum normal stress. New optimized design with straight weld joint interface reduces the stress range at 90 degree operating condition significantly. When comparing the new weld interface to original it is obvious that the angle in weld seam should be eliminated as there are high normal stresses present perpendicular to weld with original design, due to torsional loads.

Fatigue life of the boom head weld can be improved significantly by removing the weld backing. Calculations made using ENS method show significant improvement in stress levels at weld toe when the backing is removed from original boom head. Further significant improvement was achieved by topology optimizing the boom head.

Topology optimization has proven effective tool for optimizing against fatigue. Firstly the optimization was used to find new weld joint interface design. New joint design was achieved with simplified geometry and parameterized model without need of modelling each head type manually. Secondly this primary design could be optimized against fatigue to achieve significantly improved structure with relatively simple method which can be easily adapted to other structures. Simplicity of the method used here allows for fast and easy optimization of structures in early design stage.

It is clear that with careful design evaluations the fatigue life of a structure can be improved significantly. Key for thorough fatigue analysis in real life industrial applications is ease of use. Complicated and time consuming methods such as fracture mechanics are typically not used due to steep learning curve and tight design schedules in industry. Palmgren-Miner rule has been widely utilized due to its straight forward nature and ease of use and it proved here effective tool for improving the structure.

The results show that new boom head design modeled according to optimization result is significantly better than current design. It is recommended to create and take into production a new C44+ boom head similar to one shown in Figure 46. It is also recommended to use this optimization method for other cast parts in Ponsse product family to improve the fatigue resistance of the designs. If completely new design is not possible, great improvement in fatigue life can also be achieved by removing backing bar.

10.2 Uncertainties

It was observed during the project that certain input values have significant effect in the accuracy of the result. Also many assumptions had to be made to be able to define the loads acting in the structure and to generate the fatigue constraint. The uncertainties and error sources are discussed in following sections.

10.2.1 Fatigue damage model

Palmgren-Miner method is rather primitive approach for fatigue analysis. When using cumulative Palmgren-Miner formulation the fatigue life estimation is very sensitive for errors in stress values due to logarithmic nature of S-N curves. Even a small change in stress level causes significant change in the estimated fatigue life hours. This can be visualized with the function of damage sum and stress scaling factor in section 8.1.1.

The method is very sensitive and even with actual load and stress data the model would still require testing and verification to calibrate the model. Section of weld joint between cast steel boom head and steel profile should be tested against fatigue using the actual stress spectrum on test bench. These results could be used to determine S-N curve for variable amplitude loads (also called Gassner curve) and the actual damage sum for the structure.

The maximum allowable damage sum was chosen according to IIW. IIW recommendations suggest damage sum value of 0.5 for variable amplitude fatigue. (Hobbacher 2016) Studies have shown huge variation in maximum damage sum with different applications. Damage sum to failure values have been reported between 0.1 – 10. With calibration this model could be used to calculate the fatigue life of the structure with higher accuracy.

In this thesis the model was used to simulate the effect of stress range into fatigue damage in optimization and thus the actual fatigue damage is not crucial. Sensitivity of the method causes easily error when used to determine the fatigue life of the structure. In this work the aim was to improve current design and the actual fatigue life of the structure was not in our special interest. ENS stress values achieved with optimization are below the limit calculated by Palmgren-Miner rule making the design safe. The structure will last the required fatigue life of 20 000 h.

10.2.2 Stress data

Measured strain data used in this work represents only one operating condition. The load cycle and the stress spectrum can possibly be very different in eucalyptus tree fields or in steep hills. Shape of stress spectrum in different operating conditions should be analyzed and worst spectrum should be chosen to get conservative fatigue life results, applicable for all continents and environments.

Load data was used to calculate the fatigue life and the results is even at its best only rough estimation. The improvement in fatigue life can be evaluated reliably with these calculations but the absolute actual fatigue life determined in this work is a mere guess. The effects of different structural features on fatigue life of a structure are well known, but the absolute improvement in fatigue life can’t be estimated reliably.

Current knowledge of the stress state at the boom doesn’t cover possible out of phase multiaxiality. Sonsino and Kueppers propound in their work that in case of in-phase torsion and bending loads the fatigue life was four times longer in their test specimen. (Sonsino & Kueppers 2001) More sophisticated multiaxial non-proportional fatigue life estimation methods have been developed like the critical plane approach proposed by Carpinteri and Spagnoli. These methods would require defining the actual time dependent forces acting on boom head to be able to define time dependent stress state at weld root.

If the actual time dependent forces acting on boom were known, it would be possible to perform fatigue analysis using nCode design life tools. This method would result more reliable fatigue life data quickly. Biggest problem is however determining the forces. Solving the forces would be the right direction towards more reliable fatigue life assessment.

Assumption of spectrum shape at weld toe and the stress scaling made in calculations might not be representative for the structure. Assumption doesn't take into count the actual loads that caused the stress at the boom. Scaling was done using assumed worst case load condition. Scaling the stress with worst case loading into the most critical spot is assumed to results into conservative solution.

In every real life component difficulties arise also from misuse. Significant variations in fatigue lives has been observed for different operators, likely due to different working manners. Misuse yields in high peak stresses in the structure which have significant effect in the fatigue life of the structure.

10.2.3 Manufacturing flaws

Manufacturing flaws can compromise the fatigue life of the structure. In cast structures and welded structures there is always risk of harmful flaws that can lead into premature failure of the structure. The quality of the products must be improved and monitored to eliminate any quality variation in structurally critical locations such as the boom head.

With new, straight head design robot welding of the structure should be more feasible. Robot welding results into more consistent quality and should be thus implemented to crucial structures such as boom head to minimize possibility of manufacturing flaws. Currently the welding process suffers from dimensional inaccuracy of the boom spar. Before robot welding is possible the dimensional accuracy has to be improved.

New design allows visual inspection of weld root and face after welding reducing the risk of insufficiently welded structures going to customers. Joint with backing bar has to be inspected using ultrasound or other non-destructive testing method and is thus not possible to be performed on all parts.

11. FUTURE RESEARCH

New research should be made on the field of load data recovery. Current measurements made from the boom spar describe well the strain state at the location of the gauge. However this does not describe the forces acting on the boom nor the stress state at the root or toe of the weld. Any multiaxiality effects can't be determined from current measurements making fatigue life assessment less accurate. Determining the actual forces acting in the entire structure would allow us to create more complete simulation of the stress state at the weld and to simulate fatigue damage using software such as nCode.

Dynamic load data recovery would allow drastic improvement to be made on fatigue stress determination at weld toe. Using nCode virtual strain gauge or similar to determine the correct strain gauge location, field strain measurement and load data recovery with inverse method would make it possible to estimate the actual stresses at weld more accurately. Combination of load data simulation and multiaxial fatigue criterion would give more realistic description of the actual fatigue life.

Load recovery is an inverse problem which has been studied extensively. The difficulties of this type of problems have been explained by Stevens. (Stevens 1987) One of the many methods is load recovery from measured strain data, where the structure to be analyzed works as a load transducer. The behavior of the structure under loading is measured by strain gauges and the operational cycles are recorded. This recorded load cycle data is then transformed with help of FEA analysis back to load case. Inverse problems are often ill-posed and thus very sensitive to measurement errors. Investigation and utilization of these methods has been started but they still need more extensive testing and verification to prove their suitability for field testing in forest machines.

The new design improved the fatigue life of the structure beyond the requirements. This indicates that boom head could be made lighter and still fulfill the life time requirements. With the same design evaluation weight savings could be likely achieved in many other structures while maintaining or improving the fatigue life properties.

11.1 Digital twin

Era of industrial digitalization is rushing to the traditional industries. This has brought with it the idea of digital twin where the real life structure is equipped with sensors that allow real time monitoring of the structure.

This method could be implemented in Ponsse forest machine booms, by measuring cylinder pressures and boom angles real time during operation. This data could be used to

calculate the cumulative fatigue damage on time. It would make possible to create pre-service programs to prevent ultimate failure of booms.

Monitoring could also be used to better understand the usage of the booms, improve the working manners of different drivers and recognize possible miss use of the machine. The information would be also useful in possible warranty issues. System should be partly embedded into Ponsse fleet management software to allow contractor to monitor the usage of their machine and help them train their machine operators for correct operating methods.

Cycle to cycle measuring would allow us to understand the fatigue of these structures with great detail. The real load cycles to failure could be used to determine the actual cumulative fatigue damage at failure to further optimize the structures against fatigue. Active digital twin type measurement would allow Ponsse to recognize possible failures due to miss use of the machine and thus help designers to not react on failures due to excessive loading of the structures.

Creating digital twin model would require extensive investigation and work prior utilization. Writer recommends the work on this subject should be started as soon as possible. First fatigue results would not possibly be available until 2 – 3 years (14 000 - 21 000 h) after the first machine with such measurement systems is on field. Valuable information of load levels could be gathered also before fatigue results.

12. CONCLUSION

Aim of this thesis was to improve fatigue life of forest machine boom head weld joint using topology optimization. Secondary goal was to improve the manufacturability of the structure by simplifying the weld geometry.

To understand the methods and theory of fatigue life some background of the history of fatigue and the theories were explained. Different methods for fatigue life analysis of structures was explained. Special emphasis was given to weld fatigue. Most common fatigue life improvement techniques were also introduced.

Next the theory behind topology optimization was explained. The principle of penalization function was explained and the effect of penalization factor on convergence of the problem was observed with examples. Use of stress constraints on topology optimization was also explained and few examples were shown. Possible mathematical difficulties faced in typical topology optimization were also explained for better understanding of the theory. The optimization software used in this thesis was also briefly introduced.

Finally after theory the case study was introduced. Case study section consists of company and product introduction, including typical operation cycle. After brief introduction of the case study, the field measured load data is processed to obtain acceptable stress level for given fatigue life, using rainflow cycle counting and Palmgren-Miner fatigue rule. The formulation of the primary optimization problem is explained and the results are then used for final fatigue constrained topology optimization.

The optimized structure, boundary conditions and fatigue constraint function is introduced and the structure is optimized against fatigue damage. After topology optimization new 3D model of the structure is created and the structure is analyzed using FEA. Submodel of weld seam with ENS was made and analyzed. Results of optimization were finally compared against the original structure.

It was shown that using topology optimization on structures like this can be used to improve fatigue properties of a structure using current software available. New improved structure is proposed and possible error sources in analysis is discussed. Lastly some possible future research ideas are given.

REFERENCES

[1] Anderson, T.L. (2005). Fracture mechanics, 3. ed. ed. CRC Press, Boca Raton, Fla. [u.a.], 25-100 p.

[2] ASTM E 1049-85 Standard practices for cycle counting in fatigue analysis, in: (1997). Anonymous (ed.), Annual Book of ASTM Standards, Anerican Society for Testing and materials,

[3] Barsoum, Z. & Gustafsson, M. (2009). Fatigue of high strength steel joints welded with low temperature transformation consumables, Engineering Failure Analysis, Vol. 16(7), pp. 2186-2194. Available (accessed ID: 271094): http://www.sciencedirect.com/science/article/pii/S1350630709000399.

[4] Bendse, M.P. (1989). Optimal shape design as a material distribution problem, Structural Optimization, Vol. 1(4), pp. 193-202.

[5] Bendsøe, M.P. & Kikuchi, N. (1988). Generating optimal topologies in structural design using a homogenization method, Computer Methods in Applied Mechanics and Engineering, Vol. 71(2), pp. 197-224.

[6] Bhadeshia, H K D H (1999). Some phase transformations in steels, Materials Science and Technology, Vol. 15(1), pp. 22-29.

[7] Bhatti, A.A., Barsoum, Z., Mee, V.v.d., Kromm, A. & Kannengiesser, T. (2013). Fatigue Strength Improvement of Welded Structures Using New Low Transformation Temperature Filler Materials, Procedia Engineering, Vol. 66 pp. 192-201.

[8] Carpinteri, A., Spagnoli, A. & Vantadori, S. (2003). A multiaxial fatigue criterion for random loading, Fatigue and Fracture of Engineering Materials and Structures, Vol. 26(6), pp. 515-522.

[9] Champoux, R.L., Underwood, J.H. & Kapp, J.A. (1988). Analytical and experimental methods for residual stress effects in fatigue, ASTM STP, Vol. 1004

[10] Chapetti, M.D. & Jaureguizahar, L.F. (2011). Estimating the fatigue behaviour of welded joints, Procedia Engineering, pp. 959-964.

[11] Downing, S.D. & Socie, D.F. (1982). Simple rainflow counting algorithms, International Journal of Fatigue, Vol. 4(1), pp. 31-40.

[12] Duysinx, P. & Sigmund, O. (1998). New developments in handling stress constraints in optimal material distribution, 7th AIAA/USAF/NASA/ISSMO Symposium on Multidisciplinary Analysis and Optimization, pp. 1501-1509.

[13] Gross, D. & Seelig, T. (2011). Fracture mechanics with and introduction to micromechanics, 2. ed. ed. Springer, Berlin [u.a.],

[14] Harati, E., Karlsson, L., Svensson, L. & Dalaei, K. (2017). Applicability of low transformation temperature welding consumables to increase fatigue strength of welded high strength steels, International Journal of Fatigue, Vol. 97 pp. 39-47.

[15] Hobbacher, A.F. (2016). Recommendations for Fatigue Design of Welded Joints and Components, Third edition ed. Springer,

[16] Holmberg, E., Torstenfelt, B. & Klarbring, A. (2014). Fatigue constrained topology optimization, Structural and Multidisciplinary Optimization, Vol. 50(2), pp. 207-219.

[17] Holmberg, E., Torstenfelt, B. & Klarbring, A. (2013). Stress constrained topology optimization, Structural and Multidisciplinary Optimization, Vol. 48(1), pp. 33-47.

[18] Huo, L., Wang, D. & Zhang, Y. (2005). Investigation of the fatigue behaviour of the welded joints treated by TIG dressing and ultrasonic peening under variable-amplitude load, International Journal of Fatigue, Vol. 27(1), pp. 95-101.

[19] Jeong, S.H., Choi, D.-. & Yoon, G.H. (2015). Fatigue and static failure considerations using a topology optimization method, Applied Mathematical Modelling, Vol. 39(3-4), pp. 1137-1162.

[20] Kirkhope, K.J., Bell, R., Caron, L., Basu, R.I. & Ma, K.-. (1999). Weld detail fatigue life improvement techniques. Part 1: review, Marine Structures, Vol. 12(6), pp. 447-474.

[21] Krasovskyy, A. & Virta, A. (2014). Fracture Mechanics based Estimation of Fatigue Life of Welds, Procedia Engineering, Vol. 74 pp. 27-32.

[22] Lee, J.W., Yoon, G.H. & Jeong, S.H. (2015). Topology optimization considering fatigue life in the frequency domain, Computers and Mathematics with Applications, Vol. 70(8), pp. 1852-1877.

[23] Li, L. & Khandelwal, K. (2014). Two-point gradient-based MMA (TGMMA) algorithm for topology optimization, Computers and Structures, Vol. 131 pp. 34-45.

[24] Marsh, G., Wignall, C., Thies, P.R., Barltrop, N., Incecik, A., Venugopal, V. & Johanning, L. (2016). Review and application of Rainflow residue processing techniques for accurate fatigue damage estimation, International Journal of Fatigue, Vol. 82 pp. 757-765.

[25] Martinez, L.L., Peng, R.L., Blom, A.F. & Wang, D.Q. (1999). Welding and tig-dressing induced residual stresses- relaxation and influence on fatigue strength of spectrum loaded weldments, European Structural Integrity Society, Vol. 23(C), pp. 117.

[26] Matsuishi, M. & Endo, T. (1968). Fatigue of metals subjected to varying stress
, Japan Society of Mechanical Engineers,

[27] Morito, S., Nishikawa, J. & Maki, T. (2003). Dislocation density within lath martensite in Fe-C and Fe-Ni alloys, ISIJ International, Vol. 43(9), pp. 1475-1477.

[28] Moyer, J.M. & Ansell, G.S. (1975). The volume expansion accompanying the martensite transformation in iron-carbon alloys, Metallurgical Transactions A, Vol. 6(9), pp. 1785-1791.

[29] Ninic, D. & Stark, H.L. (2007). A multiaxial fatigue damage function, International Journal of Fatigue, Vol. 29(3), pp. 533-548.

[30] Nishiyama, Z. (1978). Martensitic Transformation, Academic Press, 1-13 p.

[31] Oest, J. & Lund, E. (2017). Topology optimization with finite-life fatigue constraints, Structural and Multidisciplinary Optimization, pp. 1-15.

[32] Ohta, A., Watanabe, O., Matsuoka, K., Siga, C., Nishijima, S., Maeda, Y., Suzuki, N. & Kubo, T. (1999). Fatigue strength improvement by using newly developed low transformation temperature welding material, Welding in the World, Vol. 43(6), pp. 38-42.

[33] Pedersen, M.M., Mouritsen, O.O., Hansen, M.R., Andersen, J.G. & Wenderby, J. (2010). Re-analysis of fatigue data for welded joints using the notch stress approach, International Journal of Fatigue, Vol. 32(10), pp. 1620-1626.

[34] Radaj, D., Lazzarin, P. & Berto, F. (2013). Generalised Neuber concept of fictitious notch rounding, International Journal of Fatigue, Vol. 51 pp. 105-115.

[35] Radaj, D., Sonsino, C.M. & Fricke, W. (2006). Fatigue Assessment of Welded Joints by Local Approaches: Second Edition, 1-639 p.

[36] Roy, S., Fisher, J.W. & Yen, B.T. (2003). Fatigue resistance of welded details enhanced by ultrasonic impact treatment (UIT), International Journal of Fatigue, Vol. 25(9-11), pp. 1239-1247.

[37] Schijve, J. (2012). Fatigue predictions of welded joints and the effective notch stress concept, International Journal of Fatigue, Vol. 45 pp. 31-38.

[38] Schijve, J. & Yarema, S.Y. (2003). Fatigue of structures and materials in the 20th century and the state of the art, Materials Science, Vol. 39(3), pp. 307-333.

[39] Schmit, L.A. (1960). Structural design by systematic synthesis, pp. 105-122.

[40] Schulze, V., Bleicher, F., Groche, P., Guo, Y.B. & Pyun, Y.S. (2016). Surface modification by machine hammer peening and burnishing, CIRP Annals - Manufacturing Technology, Vol. 65(2), pp. 809-832.

[41] Schütz, W. (1996). A history of fatigue, Engineering Fracture Mechanics, Vol. 54(2), pp. 263-300.

[42] Sigmund, O. & Petersson, J. (1998). Numerical instabilities in topology optimization: A survey on procedures dealing with checkerboards, mesh-dependencies and local minima, Structural Optimization, Vol. 16(1), pp. 68-75.

[43] Sonsino, C.M. (2009a). Effect of residual stresses on the fatigue behaviour of welded joints depending on loading conditions and weld geometry, International Journal of Fatigue, Vol. 31(1), pp. 88-101.

[44] Sonsino, C.M. (2009b). Effect of residual stresses on the fatigue behaviour of welded joints depending on loading conditions and weld geometry, International Journal of Fatigue, Vol. 31(1), pp. 88-101.

[45] Sonsino, C.M. (2007). Fatigue testing under variable amplitude loading, International Journal of Fatigue, Vol. 29(6), pp. 1080-1089.

[46] Sonsino, C.M., Fricke, W., De Bruyne, F., Hoppe, A., Ahmadi, A. & Zhang, G. (2012). Notch stress concepts for the fatigue assessment of welded joints - Background and applications, International Journal of Fatigue, Vol. 34(1), pp. 2-16.

[47] Sonsino, C.M. & Kueppers, M. (2001). Multiaxial fatigue of welded joints under constant and variable amplitude loadings, Fatigue and Fracture of Engineering Materials and Structures, Vol. 24(5), pp. 309-327.

[48] Stenberg, T., Barsoum, Z. & Balawi, S.O.M. (2015). Comparison of local stress based concepts — Effects of low-and high cycle fatigue and weld quality, Engineering Failure Analysis, Vol. 57 pp. 323-333.

[49] Stevens, K.K. (1987). Force identification problems - An overview
, Proceeding of the 1987 Sem Spring Conference,

[50] Suominen, L., Khurshid, M. & Parantainen, J. (2013). Residual Stresses in Welded Components Following Post-weld Treatment Methods, Procedia Engineering, Vol. 66 pp. 181-191.

[51] Trufiakov, V.I., Mikheev, P.P., Kudryavtsev, Y.F. & Statnikov, E.S. (1995). Ultrasonic Impact Treatment of Welded Joints
, IIW Doc, XIII-1609-95, pp. 1-6.

[52] Vanderplaats, G.N. (1987). Numerical Optimization Techniques, in: Mota Soares, C.A. (ed.), Computer Aided Optimal Design: Structural and Mechanical Systems, Springer Berlin Heidelberg, Berlin, Heidelberg, pp. 197-239.

[53] Webster, G.A. & Ezeilo, A.N. (2001). Residual stress distributions and their influence on fatigue lifetimes, International Journal of Fatigue, Vol. 23(SUPPL. 1), pp. S383.

[54] Yildirim, H.C., Marquis, Gary B., Prof., Aalto University,Department of Applied Mechanics, Finland, Insinritieteiden korkeakoulu, School of Engineering, Sovelletun mekaniikan laitos, Department of Applied Mechanics, Mechanics of Materials, Aaltoyliopisto & Aalto University (2013). Design aspects of high strength steel welded structures improved by high frequency mechanical impact (HFMI) treatment, Aalto University.

[55] Yonemura, M., Osuki, T., Terasaki, H., Komizo, Y., Sato, M. & Toyokawa, H. (2006). Two-dimensional time-resolved X-ray diffraction study of directional solidification in steels, Materials Transactions, Vol. 47(9), pp. 2292-2298.

APPENDIX A – STRESS SPECTRA OF ONE STRAIN GAUGE

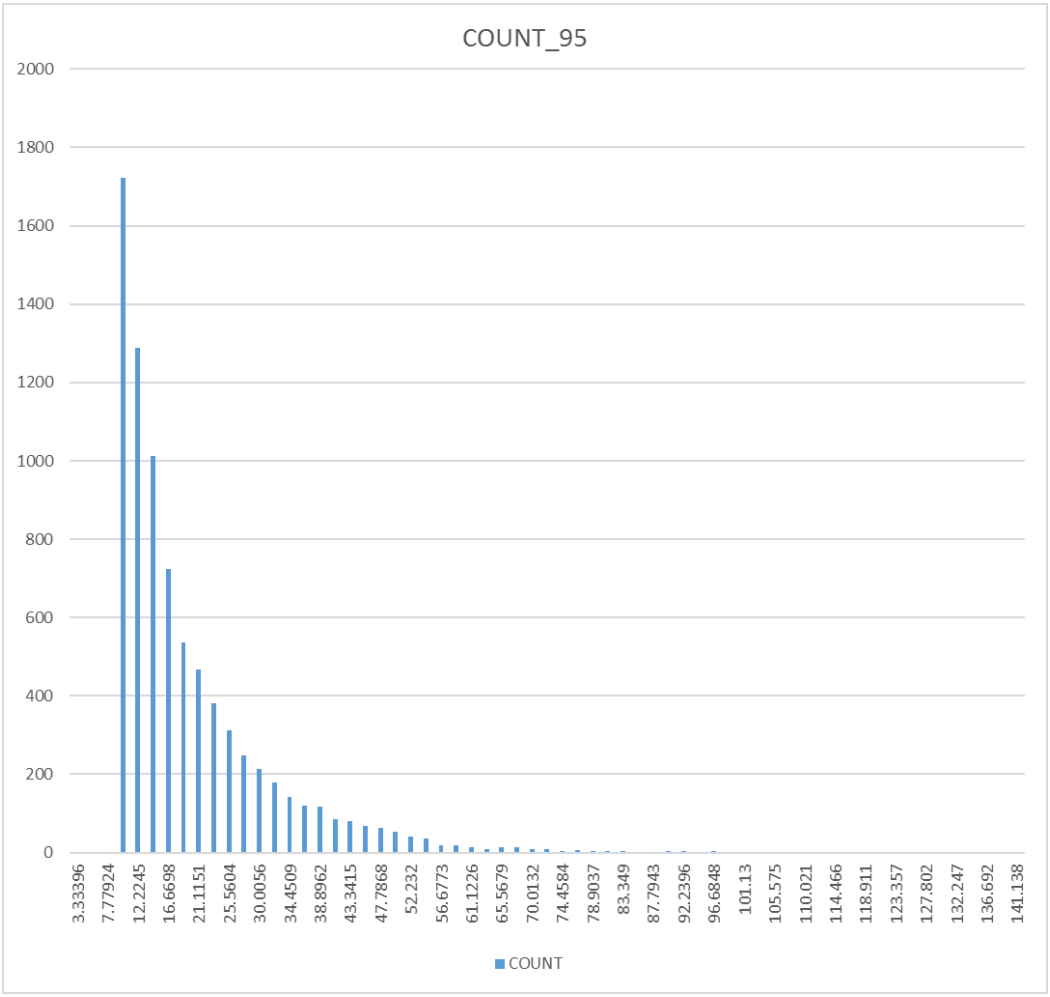

APPENDIX B – SAMPLE OF FOUR MEASURED STRESS-TIME SIGNALS